

## Comparison of fin whale 20 Hz call detections by deep-water mobile autonomous and stationary recorders

Selene Fregosi, Danielle V. Harris, Haruyoshi Matsumoto, et al.

Citation: *The Journal of the Acoustical Society of America* **147**, 961 (2020); doi: 10.1121/10.0000617

View online: <https://doi.org/10.1121/10.0000617>

View Table of Contents: <https://asa.scitation.org/toc/jas/147/2>

Published by the [Acoustical Society of America](#)

---

### ARTICLES YOU MAY BE INTERESTED IN

[Lombard effect: Minke whale boing call source levels vary with natural variations in ocean noise](#)

*The Journal of the Acoustical Society of America* **147**, 698 (2020); <https://doi.org/10.1121/10.0000596>

[Fin whale acoustic presence and song characteristics in seas to the southwest of Portugal](#)

*The Journal of the Acoustical Society of America* **147**, 2235 (2020); <https://doi.org/10.1121/10.0001066>

[Near real-time marine mammal monitoring from gliders: Practical challenges, system development, and management implications](#)

*The Journal of the Acoustical Society of America* **148**, 1215 (2020); <https://doi.org/10.1121/10.0001811>

[Repeated downsweep vocalizations of the Araguaian river dolphin, \*Inia araguaiaensis\*](#)

*The Journal of the Acoustical Society of America* **147**, 748 (2020); <https://doi.org/10.1121/10.0000624>

[Multi-year occurrence of sei whale calls in North Atlantic polar waters](#)

*The Journal of the Acoustical Society of America* **147**, 1842 (2020); <https://doi.org/10.1121/10.0000931>

[Effects of multiple exposures to pile driving noise on harbor porpoise hearing during simulated flights—An evaluation tool](#)

*The Journal of the Acoustical Society of America* **147**, 685 (2020); <https://doi.org/10.1121/10.0000595>

---



**Advance your science and career  
as a member of the**

**ACOUSTICAL SOCIETY OF AMERICA**

LEARN MORE



## Comparison of fin whale 20 Hz call detections by deep-water mobile autonomous and stationary recorders

Selene Fregosi,<sup>1,a)</sup> Danielle V. Harris,<sup>2</sup> Haruyoshi Matsumoto,<sup>1</sup> David K. Mellinger,<sup>1</sup> Christina Negretti,<sup>3</sup> David J. Moretti,<sup>4</sup> Stephen W. Martin,<sup>5</sup> Brian Matsuyama,<sup>5</sup> Peter J. Dugan,<sup>6</sup> and Holger Klinck<sup>6,b)</sup>

<sup>1</sup>Cooperative Institute for Marine Resources Studies, Oregon State University and National Oceanic and Atmospheric Administration Pacific Marine Environmental Laboratory, 2030 Southeast Marine Science Drive, Newport, Oregon 97365, USA

<sup>2</sup>Centre for Research into Ecological and Environmental Modelling, University of St Andrews, St Andrews, Fife, United Kingdom

<sup>3</sup>Department of Animal and Rangeland Sciences, College of Agricultural Sciences, Oregon State University, Corvallis, Oregon 97331, USA

<sup>4</sup>Naval Undersea Warfare Center, Newport, Rhode Island 02841, USA

<sup>5</sup>National Marine Mammal Foundation, San Diego, California 92106, USA

<sup>6</sup>Center for Conservation Bioacoustics, Cornell Lab of Ornithology, Cornell University, Ithaca, New York 14850, USA

### ABSTRACT:

Acoustically equipped deep-water mobile autonomous platforms can be used to survey for marine mammals over intermediate spatiotemporal scales. Direct comparisons to fixed recorders are necessary to evaluate these tools as passive acoustic monitoring platforms. One glider and two drifting deep-water floats were simultaneously deployed within a deep-water cabled hydrophone array to quantitatively assess their survey capabilities. The glider was able to follow a pre-defined track while float movement was somewhat unpredictable. Fin whale (*Balaenoptera physalus*) 20 Hz pulses were recorded by all hydrophones throughout the two-week deployment. Calls were identified using a template detector, which performed similarly across recorder types. The glider data contained up to 78% fewer detections per hour due to increased low-frequency flow noise present during glider descents. The glider performed comparably to the floats and fixed recorders at coarser temporal scales; hourly and daily presence of detections did not vary by recorder type. Flow noise was related to glider speed through water and dive state. Glider speeds through water of 25 cm/s or less are suggested to minimize flow noise and the importance of glider ballasting, detector characterization, and normalization by effort when interpreting glider-collected data and applying it to marine mammal density estimation are discussed. © 2020 Acoustical Society of America.

<https://doi.org/10.1121/10.0000617>

(Received 19 July 2019; revised 2 December 2019; accepted 6 January 2020; published online 10 February 2020)

[Editor: Aaron M. Thode]

Pages: 961–977

### I. INTRODUCTION

Passive acoustic monitoring (PAM) is an efficient and cost-effective tool for studying vocal marine mammal species (Mellinger *et al.*, 2007). PAM has been extensively used to study marine mammal behavior (Barlow *et al.*, 2018; Stimpert *et al.*, 2015), identify critical habitats (Yack *et al.*, 2013), understand seasonal migrations (Guazzo *et al.*, 2017), estimate animal density and abundance (Hildebrand *et al.*, 2015; Norris *et al.*, 2017), and facilitate mitigation and management of populations sensitive to human impacts (Van Parijs *et al.*, 2009). Various PAM methods exist, including fixed autonomous and cabled systems (Ioup *et al.*, 2016; Jarvis *et al.*, 2014; Wiggins and Hildebrand, 2007), ship-towed hydrophone arrays (von Benda-Beckmann *et al.*, 2010; Miller and Tyack, 1998; Rankin *et al.*, 2008), and more recently, a range of mobile autonomous platforms

(Verfuss *et al.*, 2019). These include subsurface floats and gliders (Baumgartner *et al.*, 2018; Klinck *et al.*, 2012; Matsumoto *et al.*, 2013), surface drifters (Barlow *et al.*, 2018; Lillis *et al.*, 2018), and autonomous surface vehicles (Bittencourt *et al.*, 2018; Klinck *et al.*, 2016).

Fixed, or bottom-moored, recorders are perhaps the most widely used instrument for marine mammal research. Both autonomous and cabled fixed recorders enable users to collect long-term datasets (months to years in duration), can be deployed in remote areas, record at night and in poor weather conditions, and are not known to affect the behavior of the animal of interest (Mellinger *et al.*, 2007). They are generally very quiet systems, designed to reduce self-noise (Sousa-Lima *et al.*, 2013). They are typically the least expensive PAM method, and use is widespread (Lammers *et al.*, 2008; Mellinger *et al.*, 2007; Sousa-Lima *et al.*, 2013). Cabled systems can provide data in near-real-time and over decades, allowing for both immediate and long-term monitoring (Van Parijs *et al.*, 2009). However, cabled systems are expensive and so are more typically deployed

<sup>a)</sup>Electronic mail: selene.fregosi@oregonstate.edu, ORCID: 0000-0002-2685-3736.

<sup>b)</sup>ORCID: 0000-0003-1078-7268.

by governments or large organizations and are restricted to those organizations' areas of interest (Barnes *et al.*, 2007; Mellinger *et al.*, 2007; Sousa-Lima *et al.*, 2013). Arrays of multiple fixed recorders allow for tracking and identifying individual vocalizing animals (Hatch *et al.*, 2012; Helble *et al.*, 2016). Advances in statistical methodologies have allowed for estimation of animal abundance and density from a variety of fixed recorder configurations (Marques *et al.*, 2009; Marques *et al.*, 2013). Autonomous fixed recorders have provided invaluable information on changes in marine mammal populations (e.g., Davis *et al.*, 2017).

The major limitation to a single fixed recorder is the limited spatial coverage. Spatial coverage of any recorder varies with the local sound propagation and ambient sound conditions and by the amplitude and frequency of the target sound (Helble *et al.*, 2013b; Mellinger *et al.*, 2007; Širović *et al.*, 2007; Ward *et al.*, 2011; Zimmer *et al.*, 2008). Lower frequency (<1 kHz) signals are potentially detectable over tens to hundreds of kilometers (Širović *et al.*, 2007; Stafford *et al.*, 2007) while higher frequency signals may only be detectable a few kilometers away or less (Zimmer *et al.*, 2008). Both natural and human-generated noise (from ships, weather, etc.) may mask calls of interest and further reduce the detection range (Helble *et al.*, 2013a; Stafford *et al.*, 2007; Ward *et al.*, 2011). A large array of instruments can be deployed to cover a greater survey area, including diverse habitats; however, this increases costs and processing the huge quantities of collected data (often many tens of terabytes) can be challenging (Lammers *et al.*, 2008; Van Parijs *et al.*, 2009; Roch *et al.*, 2016; Sousa-Lima *et al.*, 2013).

Ship-towed acoustic recorders are also commonly used for marine mammal surveys. These mobile systems provide better spatial coverage than fixed instruments (Mellinger *et al.*, 2007). They can combine visual and acoustic observations allowing identification of species-specific sounds (Rankin *et al.*, 2007; Rankin and Barlow, 2005), or linking of acoustic and surface behavior (Miller and Tyack, 1998). Towed recorders can provide information on important habitat (Yack *et al.*, 2013) and have the advantage of providing data in real-time (Van Parijs *et al.*, 2009). Like fixed arrays, towed arrays can be used to track vocalizing animals (Thode, 2004), identify calling individuals (Quick and Janik, 2012), and estimate animal abundance or density using a distance sampling framework (Buckland *et al.*, 2001; Norris *et al.*, 2017).

Ship-based instruments also have their disadvantages, primarily limited temporal coverage. Surveys typically last only a few weeks due to the high cost of ship operations over extended time periods (Mellinger and Barlow, 2003; Mellinger *et al.*, 2007). Surveys are limited by weather conditions and seasonal accessibility to an area (Mellinger and Barlow, 2003; Mellinger *et al.*, 2007; Norris *et al.*, 2012). Ships generate low-frequency noise and ship-towed arrays generate low-frequency flow noise as they move through the water which may mask low-frequency vocalizing baleen whale species (Barlow *et al.*, 2008; Mellinger and Barlow, 2003; Thode, 2004). Last, ship presence and associated

vessel noise may alter the vocal behavior of the animals of interest (e.g., Guerra *et al.*, 2014; Holt *et al.*, 2009; Lesage *et al.*, 1999), and echosounders have been found to influence the vocal behavior of beaked whales (Cholewiak *et al.*, 2017).

Over the past few decades, two types of deep-water mobile autonomous platforms, gliders and profiling floats, have been developed for oceanographic research (Roemmich *et al.*, 2009; Rudnick *et al.*, 2004). They provide *in situ* measurements of temperature, salinity, oxygen, currents, and many other metrics (Roemmich *et al.*, 2009; Rudnick *et al.*, 2004). They can provide processed data in near real-time via satellite connection (Roemmich *et al.*, 2009; Rudnick *et al.*, 2004). These low power platforms can cover large, otherwise inaccessible areas and be deployed for weeks to months at a time, providing data across both large spatial and temporal scales at an intermediate cost to cabled or ship-based systems (Roemmich *et al.*, 2009; Rudnick *et al.*, 2004).

Two such instruments are the Seaglider<sup>TM</sup> (Kongsberg Underwater Technologies, Inc., Lynnwood, Washington, USA) and the QUEphone, an acoustically equipped APEX float (Teledyne Webb Research, North Falmouth, Massachusetts, USA). The Seaglider is remotely piloted using Iridium satellite communications to transit between specified waypoints or along a defined heading. It dives up and down in the water column, to maximum depths of 1000 m, through small changes in buoyancy created by pumping oil in and out of an external bladder. Pump operation can be adjusted to change vertical speed and thrust. Roll and pitch are altered through lateral and rotational movement of internal batteries. Dive cycles typically last 4–6 h, with brief surface intervals for communication with a shore station. The QUEphone is capable of descending to 1500 m. Once the platform reaches the programmed depth, it drifts passively with the currents. Like the Seaglider, depth is controlled through small changes in buoyancy created by expansion or contraction of an external bladder. Dive cycles typically last 24 h, and dive depth and timing can be controlled remotely via Iridium satellite communication.

More recently, gliders and floats have been outfitted with a variety of passive acoustic recorders (Baumgartner and Fratantoni, 2008; Klinck *et al.*, 2012; Küsel *et al.*, 2017; Matsumoto *et al.*, 2006; Moore *et al.*, 2007; Van Uffelen *et al.*, 2017). Several studies have demonstrated the ability of such platforms to record and detect many marine mammal species (Baumgartner *et al.*, 2013; Klinck *et al.*, 2016; Küsel *et al.*, 2017; Matsumoto *et al.*, 2013), including near-real-time observations (Baumgartner *et al.*, 2013; Davis *et al.*, 2016; Klinck *et al.*, 2012). Surveys have included off-shore regions that are otherwise difficult to study (Burnham *et al.*, 2019; Nieuwkerk *et al.*, 2016).

Mobile autonomous platforms provide intermediate temporal and spatial coverage between fixed and ship-based PAM methods (Verfuss *et al.*, 2019). Thus far, battery and storage constraints have limited deployments to four months or less, depending on the platform, instrumentation, and survey specifications, but there is potential for improvements in capacity (Cauchy *et al.*, 2018; Klinck *et al.*, 2015; Mellinger

*et al.*, 2017). Although a glider moves much slower than a ship ( $\sim 1/2$  knot; Rudnick *et al.*, 2004), and a profiling float's movement is current driven and so can be difficult to control or predict (Roemmich *et al.*, 2009), the area surveyed by these mobile autonomous platforms extends beyond what is possible with a fixed recorder.

However, the vertical and horizontal movement of gliders and floats present potential challenges and special considerations for collecting and interpreting data, compared to traditional PAM methods. The ability of any acoustic system to record and detect a sound of interest depends on the recording system hardware and software (Mellinger *et al.*, 2007), the survey environment (Helble *et al.*, 2013b; Küsel *et al.*, 2011), and the analysis process (Leroy *et al.*, 2018; Marques *et al.*, 2013; Širović, 2016). Specifically, hardware and software limits, detector performance, and survey effort must be quantified for each recording system before meaningful interpretation of the collected data is possible. Unique operational aspects of gliders and floats may affect detector performance and how survey effort is defined.

Generally, detector performance can be influenced by (a) transient platform self-noise that triggers a false positive detection and (b) sustained platform-generated flow noise and/or increased ambient noise conditions which may lead to excessive missed detections (Helble *et al.*, 2013a; Leroy *et al.*, 2018; Ward *et al.*, 2011). Autonomous mobile platforms may be more prone than other platforms to false positive detections. Glider and float buoyancy adjustments are made via a loud, motorized pump (Matsumoto *et al.*, 2015; Roemmich *et al.*, 2009; Rudnick *et al.*, 2004), and the glider's flight path is controlled by changes in the glider's pitch or roll orientation via motor-driven changes in the center of mass (Matsumoto *et al.*, 2015; Rudnick *et al.*, 2004). Additionally, Seagliders are operated at speeds that correspond to large Reynolds numbers (very approximately, the velocity times length divided by fluid kinetic viscosity) of 350 000 to 600 000 (Rudnick, 2004). Motion or flow within any fluid becomes turbulent when the Reynolds number is sufficiently large, and turbulent flow introduces low-frequency noise as low-frequency pressure waves. This flow noise has been documented previously on acoustically equipped Seagliders (Matsumoto *et al.*, 2015; dos Santos *et al.*, 2016).

Defining survey effort for a mobile platform is more complicated than a fixed recorder or towed array. Total survey effort for a mobile platform can be considered in terms of the area covered and the time spent monitoring (Marques *et al.*, 2013). For a glider or float, survey effort in the time domain is dependent not only on the sampling regime and duty cycle, but also operational differences such as surfacing periods and depth or dive state dependent operation of the recorder. In the space domain, survey effort depends on the platform's velocity and its maximum detection radius. Within a maximum detection radius, target signals will be detected with some probability, which is often a function of range—i.e., calling animals further away will tend to be more difficult to detect (Marques *et al.*, 2013). Quantifying

differences in the detection probability becomes increasingly complex for a vertically and horizontally moving platform as detection range may be altered by the sound propagation environment (Helble *et al.*, 2013b) as it changes with platform depth or location, or platform-induced flow noise (Matsumoto *et al.*, 2015).

These variables all have the potential to influence a recording system's performance, and thus the interpretation of data collected by that system. But to date, no thorough comparison of detection capabilities between fixed or ship-towed recorders and deep-water autonomous mobile recorders has been performed. Such comparisons are necessary across a range of marine mammal sound types to gain a better understanding of the advantages and limitations of these mobile platforms as PAM systems, enable comparison with historical data sets, and ultimately estimate animal abundance and density (Marques *et al.*, 2013; Thomas and Marques, 2012; Verfuss *et al.*, 2019).

Here we present a comparative study of system performance detecting a low-frequency marine mammal call for two types of deep-water autonomous mobile platforms and a fixed seafloor hydrophone array. One acoustically equipped glider (Seaglider) and two acoustically equipped profiling floats (QUEphone) were deployed simultaneously in the vicinity of a well-studied stationary hydrophone array at the Southern California Offshore Range (SCORE) (Jarvis *et al.*, 2014). We used an automated detector to quantify the presence of fin whale, *Balaenoptera physalus*, 20-Hz pulses (Watkins *et al.*, 1987) in data collected from the three recorder types. (Another species detected, Cuvier's beaked whales, *Ziphius cavirostris*, will be the subject of future analyses.) We compared detector performance, total calls detected, hourly detection rates, and hourly and daily presence and absence of calls across the recorder types. For the glider, we examined how detection rates changed with platform movement and platform-induced noise levels. Finally, we provide recommendations for future steps to improve and expand applications of mobile autonomous vehicles for marine mammal research.

## II. METHODS

### A. Acoustic systems

The Wideband Intelligent Signal Processor and Recorder (WISPR), commercially available from Embedded Ocean Systems, Inc. (Seattle, Washington USA), has been integrated into both the Seaglider and QUEphone. WISPR receives signals via a single omni-directional hydrophone (HTI-92-WB, High Tech Inc., Gulfport, Mississippi, USA; sensitivity:  $-175$  dB re  $1\text{ V}/\mu\text{Pa}$   $\pm 3$  dB frequency response from 2 Hz to 50 kHz). A frequency-dependent gain curve, which approximately matches the inverse of the typical deep-water ambient sound profile, is applied prior to digitization (see Matsumoto *et al.*, 2015). The analog signal is recorded at a 125 kHz sampling rate with 16-bit resolution and compressed using the Free Lossless Audio Codec (FLAC). The recording system on both the glider and float



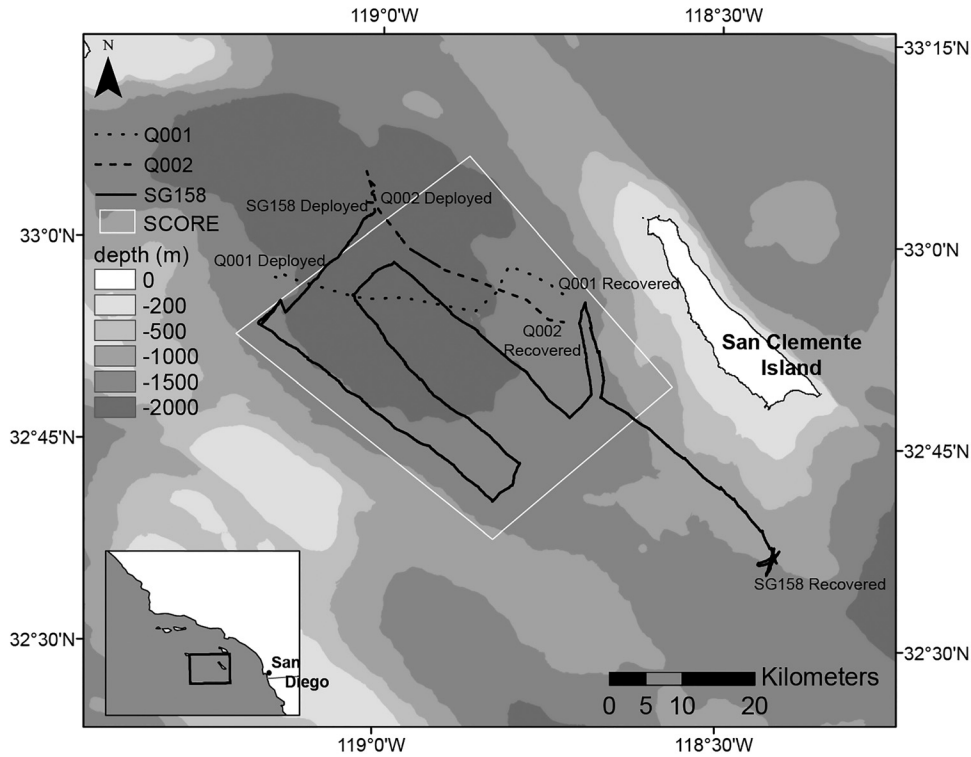


FIG. 1. Map of platform paths, the outline of the Southern California Offshore Range (SCORE) enclosing the locations of the bottom-moored hydrophones, and seafloor bathymetry in the deployment area. The Seaglider, SG158 (solid line), was deployed on the NE side of the range, and then transited across the range according to pre-planned waypoints. Q001 (dotted line) and Q002 (dashed line) were deployed along the north edge of the range, about 17 km apart, and drifted to the SE. The SCORE hydrophones are generally evenly spaced across the range (within the white solid box), with each hydrophone approximately 4 km apart.

operates continuously and can be programmed to turn on and off at a specified depth. Depth limits can also be modified remotely via Iridium satellite communication during a deployment.

The Marine Mammal Monitoring on Navy Ranges system (M3R) (Jarvis *et al.*, 2014) connects to an extensive cabled, bottom-mounted hydrophone array operated by the U.S. Navy at SCORE, approximately 150 km northwest of San Diego off the western shore of San Clemente Island in the San Nicolas Basin. The array of 178 hydrophones is typically used for tracking underwater vehicles and also provides input data to the M3R system which is capable of recording, detecting, and localizing marine mammal vocalizations (Ierley and Helble, 2016; Jarvis *et al.*, 2014; Moretti *et al.*, 2016). The hydrophones are moored near the seafloor at depths from 800 to 1800m and spaced approximately

4 km apart. The bandwidth of the subset of 79 hydrophones used in this study is from ~50 Hz to 50 kHz, but are useable down to 20 Hz (Jarvis *et al.*, 2014; Moretti *et al.*, 2016). The M3R system records the SCORE array at a sample rate of 96 kHz and 16-bit resolution in a packet format; data can also be processed and viewed in real-time (Jarvis *et al.*, 2014; Moretti *et al.*, 2016).

### B. Field deployment

One acoustic Seaglider (SG158) and two QUEphones (Q001 and Q002) were deployed on 22 December 2015 just north of SCORE for a performance comparison with the M3R system (Fig. 1 and Table I). The glider surveyed the area in evenly spaced (~10 km) transects, repeatedly diving to 1000 m depth (Fig. 2). The QUEphones were deployed

TABLE I. Deployment and recording durations for each recorder. Deployment and recovery times for M3R are the times hydrophone recording started and stopped. Overlapping recording hours refers to the time periods where all recorders were deployed and the M3R system was recording. See Table II for start and stop times of the overlap periods. Hours reported for M3R are per hydrophone (with 79 hydrophones); all M3R hydrophones recorded the same duration.

Recorder	Deployed (UTC)	Recovered (UTC)	Duration (h)	Total hours recorded	Overlapping recorded hours	Distance traveled (km)	Speed (km/day)
SG158	12/22/15 2:42	1/4/2016 16:33	325.8	258.4	179.3	261.0	19.2
Q001	12/22/15 4:51	1/4/2016 20:46	327.9	300.9	200.2	47.1	3.5
Q002	12/22/15 3:16	1/4/2016 16:49	325.5	301.8	203.7	53.0	3.9
M3R (per hydrophone)	12/21/15 5:22	1/5/2016 17:24	372.0	268.4	220.0	n/a	n/a

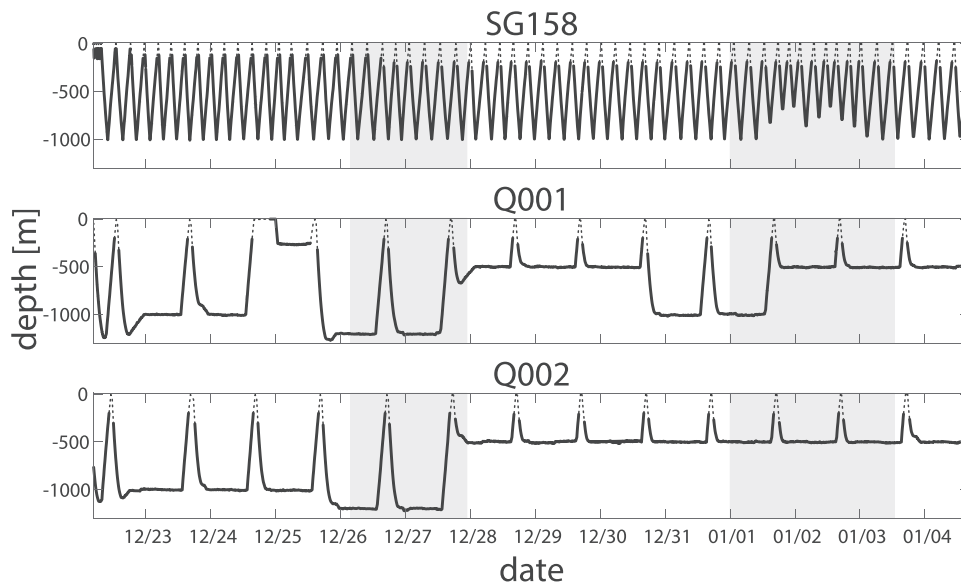


FIG. 2. Dive profiles of the Seaglider (SG158) and QUEphones (Q001 and Q002). Black solid lines indicate PAM system is on, dotted lines indicate PAM system off. Gray shaded areas indicate times when the M3R recorder was not operational and were excluded from call detection analyses.

17 km apart with the expectation that they would drift south-east in parallel to cover approximately equal areas of the SCORE range. They were initially programmed to drift at a depth of 1000 m, surfacing every 24 h (Figs. 1 and 2). However, the current systems in the Southern California Bight are complex (e.g., Bray *et al.*, 2002; Dong *et al.*, 2009; Hickey, 2003) and not easy to predict over small temporal and spatial scales. Q002 initially drifted northward and away from the range while Q001 drifted to the east across the range very slowly (Fig. 1). To change the drift direction and speed, drift depth was increased to 1200 m and then decreased to 500 m (Fig. 2), causing Q002 to reverse course and drift to the south and southeast, and causing Q001 to drift more quickly to the east.

To conserve battery and data storage space, the WISPR system on Q001, Q002, and SG158 was turned off at depths shallower than 200 m. Mid-frequency (500 Hz to 25 kHz) ambient ocean sound levels are typically higher near the surface (Hildebrand, 2009), and Cuvier’s beaked whales, a separate target species of this deployment, are known to echolocate primarily below 200 m (Johnson *et al.*, 2004). Therefore, depths above 200 m were deemed non-optimal recording conditions and the system was powered off. On SG158, the hydrophone was mounted inside the hull in the rear third of the glider, near the external buoyancy bladder. For the QUEphones, the hydrophones were mounted externally on the top, near the antenna. All mobile platforms were recovered on 4 January 2016.

Concurrent with the mobile survey, the M3R system recorded acoustic data from 79 bottom-mounted hydrophones. The 8 TB hard drives utilized for acoustic recording on the range wrote data at an insufficient speed, which caused write errors as the data drives approached capacity (after ~96 h of recording on each). This caused two major data dropouts as the first and then second disks filled, resulting in loss of approximately 100 h of data per hydrophone (out of 372 total deployment hours; Table I). To maintain uniformity in comparisons of detection abilities across all

recorder types, analyses were restricted to the periods when all three mobile systems were deployed and the SCORE array was recording properly (Table II), hereafter referred to as the overlap periods.

### C. Acoustic analyses

Initial data processing included downsampling glider and float WISPR recordings to 1 and 10 kHz sampling rates for easier viewing of the low-frequency noise and fin whale calls and converting the M3R recordings from the packet format to FLAC files using the MATLAB-based toolbox RAVEN-X (Dugan *et al.*, 2018; Dugan *et al.*, 2016).

#### 1. Call detection

A spectrogram correlation template detector (Mellinger and Clark, 2000) targeting fin whale 20 Hz pulse calls (Watkins *et al.*, 1987) was run across all datasets using the MATLAB-based toolbox RAVEN-X (Dugan *et al.*, 2018; Dugan *et al.*, 2016). The template algorithm tested three synthetic frequency sweep templates: (1) 17 to 24 Hz over ~1 s, (2) 19 to 26 Hz over ~1.25 s, and (3) 18 to 23 Hz over ~1.5 s. All template spectrograms had a 2 kHz sampling rate, 2048 sample Hann window (3 dB filter bandwidth: 1.404 Hz) with 75% overlap. For each candidate fin call, a single detection event was finalized against the template that had the highest normalized spectrogram correlation score. Call duration and

TABLE II. Start and end times of overlapping recording periods in which all mobile platforms were deployed and M3R was active but excluding periods when M3R data was not properly recorded. All detection and noise comparisons were done only during these periods.

	Start	Stop	Duration (hours)
Period 1	12/22/2015 4:51	12/26/2015 3:42	94.9
Period 2	12/27/2015 22:45	12/31/2015 23:59	97.2
Period 3	1/3/2016 12:41	1/4/2016 16:33	27.9
		Total	220.0

bandwidth were set according to the finalized template. Signal-to-noise ratio (SNR) was calculated in MATLAB using the M29 measurement from Mellinger and Bradbury (2007).

Detector performance across recorder types was evaluated through manual annotation of a subset of recordings from M3R, SG158, and Q001. A five-minute sample period was randomly selected from within every seventh hour initially, and then within every third hour to increase the sample size, resulting in samples taken from within every third to fourth hour (e.g., 0000, 0300, 0700, 1000, 1400, etc.) throughout the overlap period. These hours were selected to avoid coinciding with the timing of platform dive cycles or potential diel patterns in vocalizations. For each five-minute annotation period, a single M3R hydrophone was randomly selected for manual annotation to ensure the detector was evaluated over a spatially representative sample of M3R hydrophones. If the five-minute period fell when the glider or QUEphone's acoustic system was off (because it was at or near the surface) that hour was skipped. Fin whale 20 Hz calls (30–15 Hz, 1 s duration downsweeps) were manually annotated by an experienced analyst (CN) in RAVEN PRO 1.5 (Ithaca, New York, USA) on the 1 kHz sampling rate data using a 2048-sample Hann window (3 dB filter bandwidth: 0.702 Hz) with 95% overlap. The SNR for each manual detection was calculated the same way as the detector-generated detections, in MATLAB using the M29 measurement from Mellinger and Bradbury (2007). Manual detections were considered true detections and compared to detector outputs using custom MATLAB scripts; detections were classified as true positives if they overlapped with the manually marked call by at least 50% in both time and frequency. Visual inspection of a subset of false positives and missed detections confirmed this overlap criterion was appropriate. Precision (proportion of total detections that were correct detections), recall (proportion of true calls that were correctly detected), and false positive rate (the proportion of total detections that were incorrect detections) were calculated as outlined in Mellinger *et al.* (2016). Precision and recall were not normally distributed, so a Kruskal-Wallis test was performed to test the null hypothesis that precision and recall values for each recorder type had equal distributions. A *post hoc* Dunn's multiple comparison test on significant results identified pairwise differences.

For each recorder, detections were binned hourly and normalized by total recording minutes in that hour (hereafter referred to as detections per hour). Median detections per hour and interquartile ranges (IQR; 25%–75%) were calculated for M3R per deployment hour (median across all hydrophones) and per hydrophone (median across all deployment hours). A Kruskal-Wallis test was used to test the null hypothesis that detections per hour across all M3R hydrophones had equal distributions. Then, the closest M3R hydrophone to each mobile platform for each hour was identified by the shortest great-circle distances between each M3R hydrophone and mean latitude and longitude of the mobile platform during that hour. Because detections per hour were non-normally distributed, a Wilcoxon signed rank

test was used to test the null hypothesis that detections per hour on each mobile platform had the same distribution as the detections per hour on the closest M3R hydrophone at each hour. Exploratory analyses showed apparent higher flow noise levels during glider descents compared to ascents so glider detections per hour were categorized by dive state and again compared to the closest M3R hydrophone using a Wilcoxon signed rank test. Glider dive states were assigned using the vertical velocity measured by the glider's pressure sensor every minute. Hours with all negative vertical velocities were categorized as descents and hours with all positive vertical velocities were categorized as ascents. Hours with a mix of positive and negative vertical velocities were not included in the statistical analysis. Finally, the number of detections per hour was compared to mean platform depth per hour for the three mobile recorders. To test the null hypothesis of no correlation between the number of detections per hour and platform depth, a Spearman's rank correlation test was selected as it can account for the non-normality and unequal variance. Significance of all statistical tests was assessed at the 5% ( $p = 0.05$ ) level.

## 2. Noise levels

To examine inter and intra-recorder differences in sound levels across both frequency and time, long-term spectral average plots (LTSAs) (Wiggins and Hildebrand, 2007), with 10 s temporal and 1 Hz frequency resolution were calculated from 10 to 5000 Hz for each mobile platform. Spectral probability density (SPD) plots were created from the LTSAs following the methods outlined in Merchant *et al.* (2013). SPD is the empirical probability density of the power spectral density at each frequency. It allows examination of how sound level variation is distributed in both frequency and time in a long-term acoustic dataset (Merchant *et al.*, 2013). Median (50th), 5th, and 95th percentile levels were calculated for each mobile platform, and for the glider during ascents and descents separately, at three frequencies of interest: 12 Hz ("low flow noise"), 40 Hz ("high flow noise"), and 3000 Hz ("wind noise"). The 12 and 40 Hz frequency points were selected as indicators for low-frequency flow noise on either side of the frequency band of fin whale 20-Hz pulses. Sound levels below 50 Hz have been used previously to characterize flow noise over animal-borne acoustic recording tags (e.g., von Benda-Beckmann *et al.*, 2016; Goldbogen, 2006) and have been found to be correlated with Seaglider speed (dos Santos *et al.*, 2016), and 3000 Hz, above typical flow-noise frequencies, was selected to represent wind-driven ambient ocean noise to examine changes in sound levels over time and with glider state. A frequency of 3000 Hz has proven useful to describe surface wind in a passive acoustic glider application and in acoustic animal-borne tag recordings (von Benda-Beckmann *et al.*, 2016; Cauchy *et al.*, 2018). All noise levels reported hereafter are power spectrum density levels in dB re  $1 \mu\text{Pa}^2/\text{Hz}$ .

A regression analysis was used to explore the relationship of glider speed and orientation with low- and mid-frequency noise levels. All three power spectrum density levels were modeled against vehicle dive state as a categorical variable (ascent vs descent defined by positive or negative glider measured vertical velocity, respectively), and an estimate of speed through water and time as continuous variables, in R 3.5.3 (R Core Team, 2019). We assumed noise levels were consistent over one minute and extracted the lowest 12, 40, and 3000 Hz power spectrum density level (10 s Hann window, 0% overlap) per minute to represent noise level in that minute (to remove transient sounds). Speed through water was estimated as the vertical velocity divided by the sine of vehicle pitch. Glider vertical speed and pitch are directly measured by the glider’s sensors but are collinear with one another, so they were combined into a single simplified explanatory variable. While the glider’s on-board movement models do calculate total vehicle velocity and horizontal speed through water, those parameters have been shown to have high errors (Van Uffelen *et al.*, 2013; Van Uffelen *et al.*, 2016), so were not included. Dives 1 through 6 were excluded from the regression analysis because these were shallow trimming dives (less than 200 m) in which the glider pilot is adjusting many flight parameters to balance the glider for the *in situ* ocean conditions. Finally, noise levels and speed through water were binned every 30 min. Time was defined as the start of each 30-min bin and median values of noise level and speed through water in each bin were used to build the final regression data set (n = 500 bins). Binning was performed because the full dataset (n = 15 377 min) was too computationally expensive to model successfully. Median values were used for noise level and speed through water because minute-scale data were not always normally distributed within each 30-min bin. The full model included an interaction term between speed through water and dive state,

$$\text{noise} \sim \text{speedThroughWater} + \text{diveState} + \text{time} \\ + \text{speedThroughWater} : \text{diveState}.$$

Model fitting was conducted at each frequency band independently. Residual plots were inspected and diagnostic tests were conducted to check the assumptions of constant error variance, error independence, and normality. Cook’s distance was used to remove outliers, which corresponded to

time periods when the glider’s motors were on. These data violated assumptions of independence and equal error variance at all three frequencies. A generalized least squares model was selected because it is an extension of linear regression that allows for heteroscedasticity and non-independence by applying weighted variance and correlation structures (Zuur *et al.*, 2009). The optimal variance and correlation structures were chosen for each frequency independently using the full model and comparison of Akaike’s information criteria (AIC). Inclusion of the interaction terms and all explanatory variables was verified using a step-down procedure and comparing AIC scores. Predictions of power spectrum density levels were calculated at speeds of 13 to 31 cm/s for ascents and 24 to 53 cm/s for descents, in 1 cm/s increments, with time held constant for 12 and 40 Hz. These values were selected because they spanned the minimum and maximum speed values for each dive state, and median time was used as the constant time value. Because speed through water was not included in the final 3000 Hz model, predictions of power spectrum density at 3000 Hz were calculated at times of 0 to 12 days, in 12-h increments. Significance of all coefficients was assessed at the 5% (p = 0.05) level.

### III. RESULTS

M3R recorded 220 h per hydrophone (Table I), or 17 380 total hours on 79 hydrophones, during the 220 h of the overlapping periods (Table II). SG158 recorded 178 h, and Q001 and Q002 recorded 200 and 203 h of the overlapping periods, respectively (Table I). An LTSA of the entire deployment period for all mobile recorders can be found in supplemental Fig. 1.<sup>1</sup> The glider covered a total distance of 261 km, at an average rate of 19 km/day, while the QUEphones drifted 47 km (Q001) and 53 km (Q002) both at a rate of less than 4 km/day (Table I).

#### A. Call detection

A total of 49, 58, and 64 five-minute periods were annotated for the SG158, Q001, and M3R recordings, respectively (Table III). Overall detector performance was similar for all recorders, with median precision over 86% and median recall over 50% (Table III and Fig. 3;  $\chi^2(2) = 5.46$ , p = 0.07, and  $\chi^2(2) = 2.13$ , p = 0.34). Variability within each recorder, across five-minute sample periods, was high, with IQRs from 15% to 22%. When glider ascents and descents were treated

TABLE III. Detector performance evaluation metrics by recorder type. Precision and recall are reported as median and interquartile ranges of metrics calculated for each individual 5-min sampling period. Correct detections and missed detections are the total pooled counts across all sample periods. Total false alarms for all sample periods were normalized by total minutes sampled to get false alarms per hour. Seaglider (SG158) sample periods were further separated by dive state (ascent and descent).

Recorder	Sample periods	Precision (IQR)	Recall (IQR)	Correct detections	Missed detections	False alarms per hour
SG158	49	95.3% (20.6)	57.2% (22.6)	415	336	27.2
<i>ascent</i>	31	86.3% (40.0)	63.1% (22.7)	351	241	42.2
<i>descent</i>	18	100% (0.0)	50% (35.0)	64	95	1.3
Q001	58	87.1% (20.2)	52.4% (16.4)	813	751	29.2
M3R	64	92.5% (15.4)	50.7% (20.0)	737	754	24.4



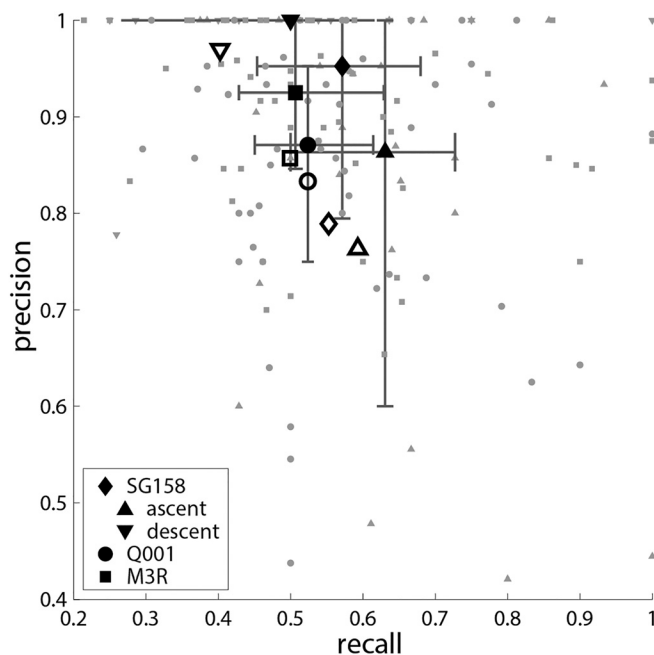


FIG. 3. Precision and recall metrics for the fin whale 20-Hz pulse detector. Small gray shapes are precision and recall rates for each individual 5-min sample period. Solid black shapes with error bars are median and interquartile range of all individually marked 5-min periods for each recorder. Open black shapes indicate overall precision and recall values calculated from pooled counts of correct detections, misses, and false alarms. SG158 is further broken down by dive state with 5-min periods during ascents as upward pointing triangles and descent periods represented by downward facing triangle.

as separate groups, precision during descents was near perfect (median 100%; almost zero false alarms) and was statistically different than the other recorders and glider ascents [ $\chi^2(3) = 22.64$ ,  $p < 0.001$ ]. Conversely, recall was elevated during glider ascents (fewer misses), compared to glider descents, Q001, and M3R, but this difference was not statistically significant. Median recall was not the same across all recorder types and glider dive states [ $\chi^2(3) = 9.02$ ,  $p = 0.03$ ], however, the *post hoc* Dunn’s multiple comparison test, which adjusts for the number of comparisons, showed no significant difference in any of the pairwise comparisons. Detection SNR distributions and results from the detector evaluation statistical tests can be found in supplemental Figs. 2–4.<sup>1</sup>

Fin whale detections were present on all days on all M3R hydrophones. Total detections per M3R hydrophone ranged from 29 093 to 46 707 (median 42 176). Median hourly detections across the deployment duration ranged from 4.0 (IQR 1.0–12.75) to 322.0 (IQR 310.5–333.0) detections per hour. Only 24 total hours, or 0.1% of total possible hours of all hydrophones, had no fin whale detections. Median detections by hydrophone, across all deployment hours, ranged from 149 (IQR 106.5 – 211.0) to 217.5 (IQR 174.0 – 264.0) detections per hour. A Kruskal-Wallis test showed that variation in median detections was significant across hydrophones [ $\chi^2(78) = 555.47$ ,  $p < 0.001$ ], with more southerly, shallower hydrophones having fewer detections (supplemental Fig. 5<sup>1</sup>).

Q001 had 39 214 and Q002 had 41 265 total detections, with detections present on all days. Q001 and Q002 had median hourly detection rates of 204.0 (IQR 152.0–246.0) and 218 (IQR 154.0–255.0) detections per hour, respectively (Fig. 4). Q002 had only one hour in which no detections were reported (0.5%). Detections per hour on Q001 were not significantly different from the detections per hour on the closest M3R hydrophone ( $Z = -0.8$ ,  $p = 0.4$ ; Fig. 4). Similarly, hourly detection counts for Q002 were not significantly different from detections per hour at the closest M3R hydrophone ( $Z = -0.7$ ,  $p = 0.5$ ; Fig. 4), or from Q001 ( $Z = -1.7$ ,  $p = 0.08$ ). Detections per hour did not correlate with platform depth for either Q001 ( $\rho = -0.113$ ,  $p = 0.1037$ ) or Q002 ( $\rho = 0.027$ ,  $p = 0.692$ ).

SG158 had a total of 20 522 detections, with detections present on all days. The median number of detections per hour was 96.3 (IQR 48.0–171.5; Fig. 4). After normalizing for recording time, six hours (2.7%) had no fin whale detections. The median number of detections per hour by the glider was less than half the median number of detections per hour by Q001 and Q002 and the closest M3R hydrophone (Q001:  $Z = -11.1$ ,  $p < 0.0001$ ; Q002:  $Z = -11.5$ ,  $p < 0.0001$ ; M3R:  $Z = -11.8$ ,  $p < 0.0001$ ; Fig. 4). When glider ascents and descents were examined separately, the median number of detections per hour during glider descents was 78% less than M3R ( $Z = -7.37$ ,  $p < 0.0001$ ) but during ascents was only 18% less than M3R ( $Z = -6.49$ ,  $p < 0.0001$ ; Fig. 4). Hourly detections did not correlate with glider depth ( $\rho = 0.095$ ,  $p = 0.187$ ). Hourly detection counts for each recorder are available in supplemental Table I.<sup>1</sup>

## B. Noise levels

Overall noise levels measured by all instruments were variable, and relatively high throughout the deployment (Table IV; Figs. 5 and 6), likely due to periods of high wind, wave, and rain activity as is typical in the winter months offshore of the Channel Islands. LTSA and SPD plots were marked by high received levels around 20 Hz, a signature of the near-constant fin whale calling activity (Figs. 5 and 6). Elevated noise levels below 60 Hz can be observed for SG158 in the LTSA (Fig. 5), particularly during descents. Sound levels across all frequencies were more variable for SG158 than Q001 or Q002 (Fig. 6). Median power spectrum density levels for all instruments were 5 to 12 dB higher at 12 Hz than 40 Hz and 17–27 dB higher at 40 Hz than 3000 Hz (Table IV and Fig. 7). Median power spectrum density levels on the glider were 15, 10, and 4 dB louder than the QUEphones at 12, 40, and 3000 Hz, respectively (Table IV and Fig. 7).

Glider ascents were generally quieter than glider descents. Ascents tended to be slower, with a steeper glider pitch angle. Mean glider speed was 9.3 (SD: 1.4) cm/s during ascents and 12.4 (SD 2.4) cm/s during descents. Glider pitch was bimodal for both ascents and descents. Ascents showed a main peak at 24° and a smaller peak at 34° (median 24.2°). Descents showed a main peak at 18° and a

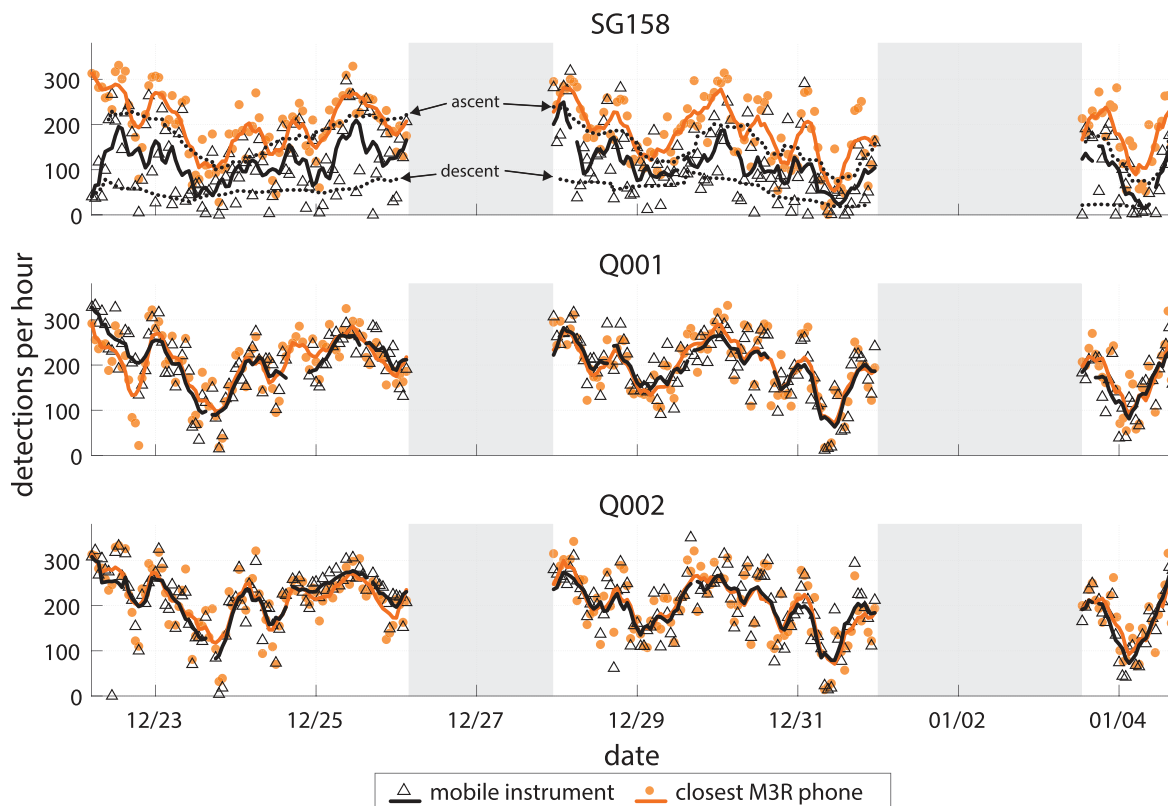


FIG. 4. (Color online) Detections per hour for each mobile platform (open triangles and solid black line) and the corresponding closest bottom-moored hydrophone (orange circles, solid orange line) during that hour. Lines represent smoothed counts over 6 h. Smoothed counts for SG158 during ascents and descents only are show as the dotted black line and indicated with arrows in the top panel.

smaller peak at 29° (median 17.9°). The steeper pitch angles that created these secondary peaks coincided with time periods when the glider was within a few km of the target waypoint where it is programmed to perform a steeper dive to not overshoot that waypoint.

Regression analysis results varied for each frequency of interest, including the optimal model and correlation structure. Exploratory and residual plots can be found in supplemental Figs. 6–14.<sup>1</sup> The independence assumption was no longer violated after applying an autocorrelation-moving average (ARMA) correlation structure of order  $p=1$  and  $q=0$  to all frequencies. Non-constant variance was accounted for at 12 and 40 Hz using an identity variance structure which allowed variance to differ by dive state. The preferred variance structure at 3000 Hz was a combined variance structure including an identity structure of dive state

and a constant-plus-power structure which allowed variance to also differ by time.

The preferred model at 12 Hz included explanatory variables for speed through water, dive state, and the interaction between speed through water and dive state, but did not include time. All explanatory variables had a significant effect on 12 Hz noise levels (Table V). During ascents 12 Hz noise levels increased 1.3 dB with every 1 cm/s increase in speed through water. During descents, 12 Hz noise levels increased only 0.65 dB per 1 cm/s increase in speed through water (Table V) but descents were generally faster, and louder, than ascents (Fig. 8). The full model was preferred at 40 Hz, with strong correlations with speed through water, dive state, and the interaction term. Time was a significant explanatory variable ( $p=0.0021$ ) but the effect was minimal ( $-0.0002$ , Table V). At 40 Hz, a 1 cm/s increase in

TABLE IV. Median (50th), 5th, and 95th percentile 12, 40, and 3000 Hz power spectrum density levels (dB re 1  $\mu\text{Pa}^2/\text{Hz}$ ; 10 s Hann window, 0% overlap) for all mobile platforms. Glider (SG158) percentiles are further separated into ascent and descent dive states.

Recorder	12 Hz				40 Hz				3000 Hz			
	95%	50%	5%	$\Delta 5-95\%$	95%	50%	5%	$\Delta 5-95\%$	95%	50%	5%	$\Delta 5-95\%$
SG158	116.4	102.1	85.0	31.4	78.1	90.0	109.1	31.0	44.5	66.4	77.6	33.1
<i>ascent</i>	106.6	97.7	83.4	23.2	76.5	87.0	108.2	31.7	44.3	66.1	76.4	32.1
<i>descent</i>	117.4	106.5	98.4	18.9	84.1	94.1	108.3	24.2	44.6	67.0	77.7	33.1
Q001	99.3	87.5	79.0	20.3	69.7	80.1	91.5	21.8	49.8	62.1	71.1	21.3
Q002	95.9	84.7	76.3	19.6	69.2	79.7	90.9	21.7	42.3	62.4	70.6	28.3

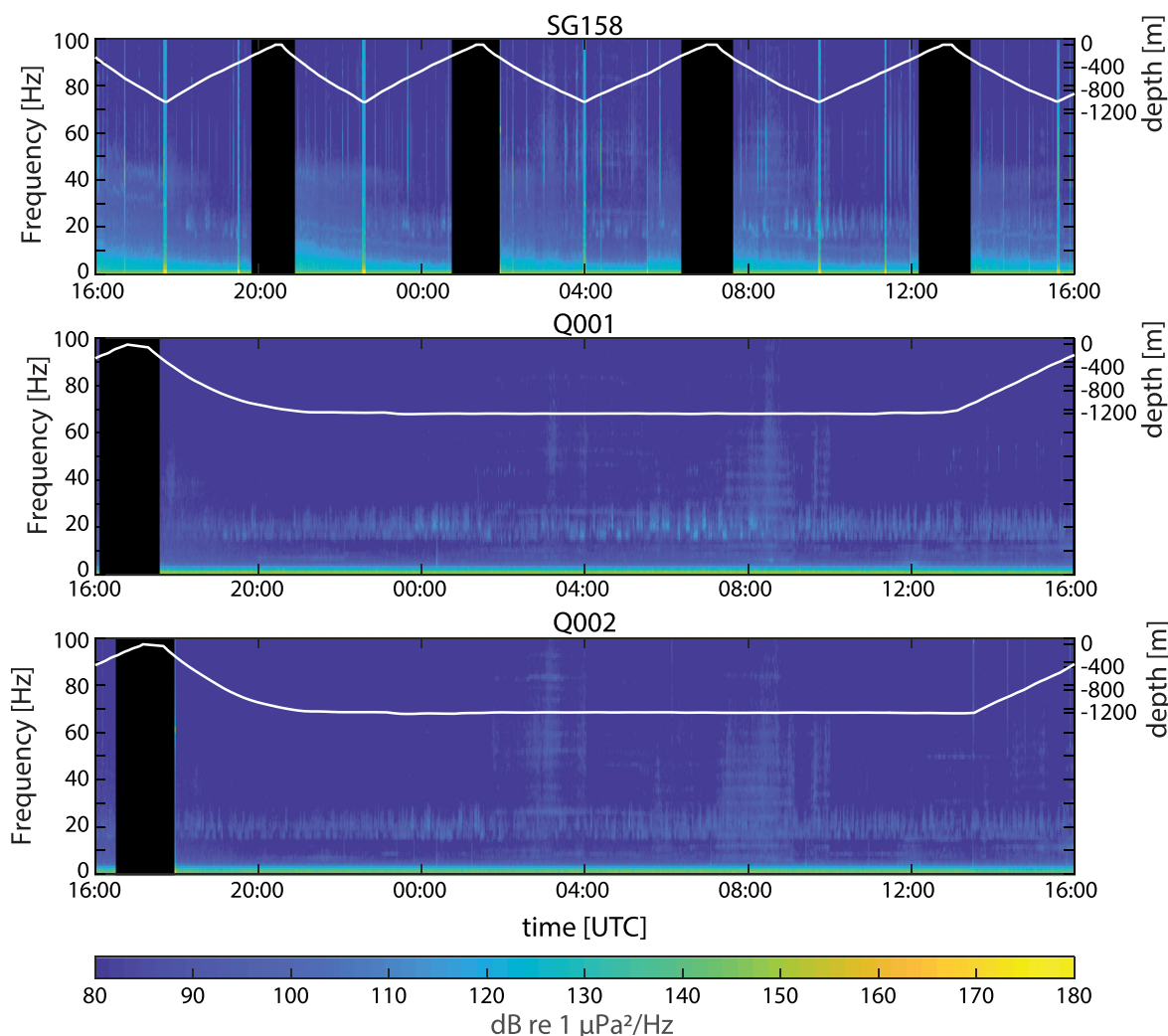


FIG. 5. (Color online) Example LTSA plot (10 s, 1 Hz) showing 24 h of acoustic data recorded by SG158, Q001, Q002 from 12/26/2015 16:00 to 12/27/2015 16:00 UTC. The white solid line and right-hand y axis indicate platform depth at the time of the acoustic recording. Black bands indicate breaks in recording when the platform was at the surface. Fin whale 20-Hz pulses are visible in the LTSA as lighter blue portions around 20 Hz. Light blue-green vertical stripes in the glider spectrogram are broadband noise caused by the glider’s buoyancy pump inflating at the bottom of each dive.

speed increased noise levels by 0.34 dB during ascents and by 0.60 dB during descents (Table V, Fig. 8). Like at 12 Hz, descents were generally louder at 40 Hz as well (Fig. 8). Only dive state and time were preferred in the best model of 3000 Hz noise levels, and time did not have a significant effect (Table V, Fig. 8). Descents were, on average, only slightly (1.5 dB) louder than ascents (Table V).

#### IV. DISCUSSION

Through analysis of recordings collected by simultaneously deployed passive acoustic recorders, we have provided validation that acoustically equipped deep-water mobile autonomous platforms such as Seagliders and QUEphones can successfully monitor low frequency marine mammal vocalizations. This study provides the first documentation of potential differences in survey capabilities of gliders and profiling floats compared to stationary bottom-mounted recorders. Overall detector performance did not vary by recorder type but was highly variable depending on

noise conditions. Fine scale temporal differences in the number of fin whale call detections by each system were related to operational differences including depth-dependent duty cycling and glider speed. Elevated glider speeds introduced flow noise in the frequency band of fin whale calls which, at times, completely masked fin whale calls. However, hourly and daily presence of fin whale call detections, as is typically reported in baleen whale monitoring surveys, were the same across all recorder types. Further, flow noise was not apparent in spectra at higher frequencies and was indeed not significant at 3000 Hz. Interestingly, number of detections per hour did not vary with mobile platform depth. This study supports future use of acoustically equipped gliders to provide intermediate spatiotemporal coverage in surveys of low-frequency vocalizing marine mammals and proposes sampling and flight considerations for future deployments.

The glider surveyed over 250 km in two weeks. It followed the designated survey plan very well, traversing the target survey area (the SCORE range) near its predicted



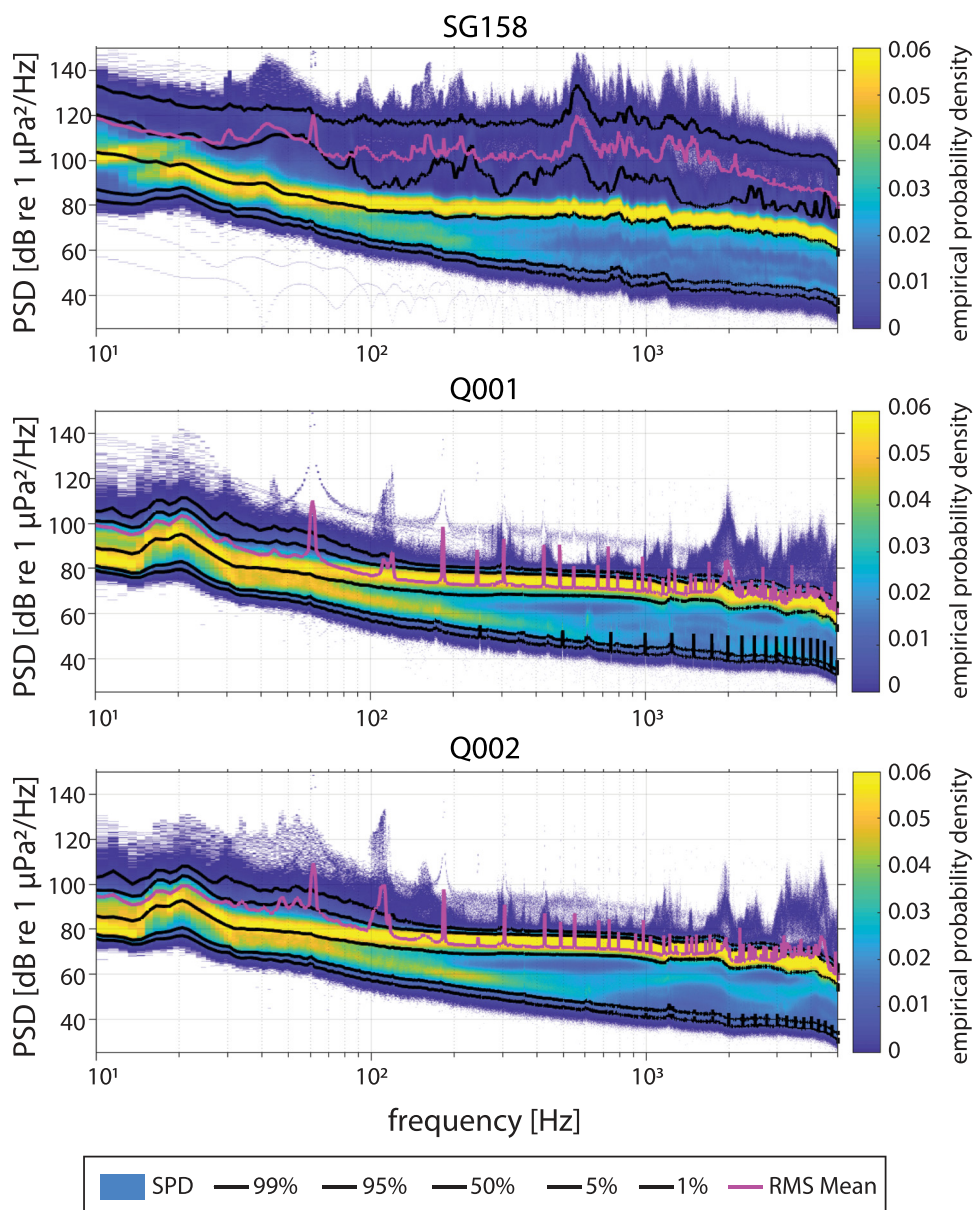


FIG. 6. (Color online) SPD plots for SG158, Q001, and Q002, up to 5 kHz, using methods outlined in Merchant *et al.* (2013) on the 10 kHz sample rate LTSA of the entire deployment calculated with a 1 Hz, 10 s Hann window for each mobile platform. Width of SPD shows variability in noise levels across the deployment duration.

speed of 20 km/day. The effects of local currents on SG158’s ability to follow its programmed track were minimal compared to other Seaglider deployments (Harris *et al.*, 2017). This supports that control of a Seaglider is sufficient to set up and conduct a design-based survey with defined transects (Buckland *et al.*, 2001; Harris *et al.*, 2017; Verfuss *et al.*, 2019) and *et al.*, 2001; Verfuss *et al.*, 2019). Conversely, drift speed and direction of the QUEphones were depth-dependent and difficult to predict. For example, while Q001 and Q002 were deployed only 17 km apart both drift speed and direction of each varied over the deployment duration. Although both floats eventually drifted onto SCORE, they spent considerably less time recording in the target survey area compared to the glider. Relying on a drifting platform to follow a planned survey track may be risky unless the currents of the area are well-documented and understood. While it may be possible to follow survey design principles (e.g., Buckland *et al.*, 2001) to deploy an

array of drifting recorders to cover a representative portion of a larger study area (e.g., Griffiths and Barlow, 2016), the survey design cannot always be ensured.

Total hours recorded by the glider and both QUEphones did not equal the total time they were at sea, nor the total hours recorded by the M3R system. The glider and QUEphone had fewer total recorded hours than the M3R system because the PAM system was shut off at depths shallower than 200 m to preserve battery and storage space (Fig. 2 and supplemental Fig. 1—black bars<sup>1</sup>). This duty cycle was specific to this deployment, the dive cycle durations for the glider and QUEphones, and the WISPR recording system. The difference in recording time across recorders was easily quantified by normalizing call counts by recording duration. PAM system operation can be adjusted to operate almost continuously (excluding surface intervals) or at any duty cycle desired, and in future work call counts could be normalized accordingly. Additionally, call counts may need



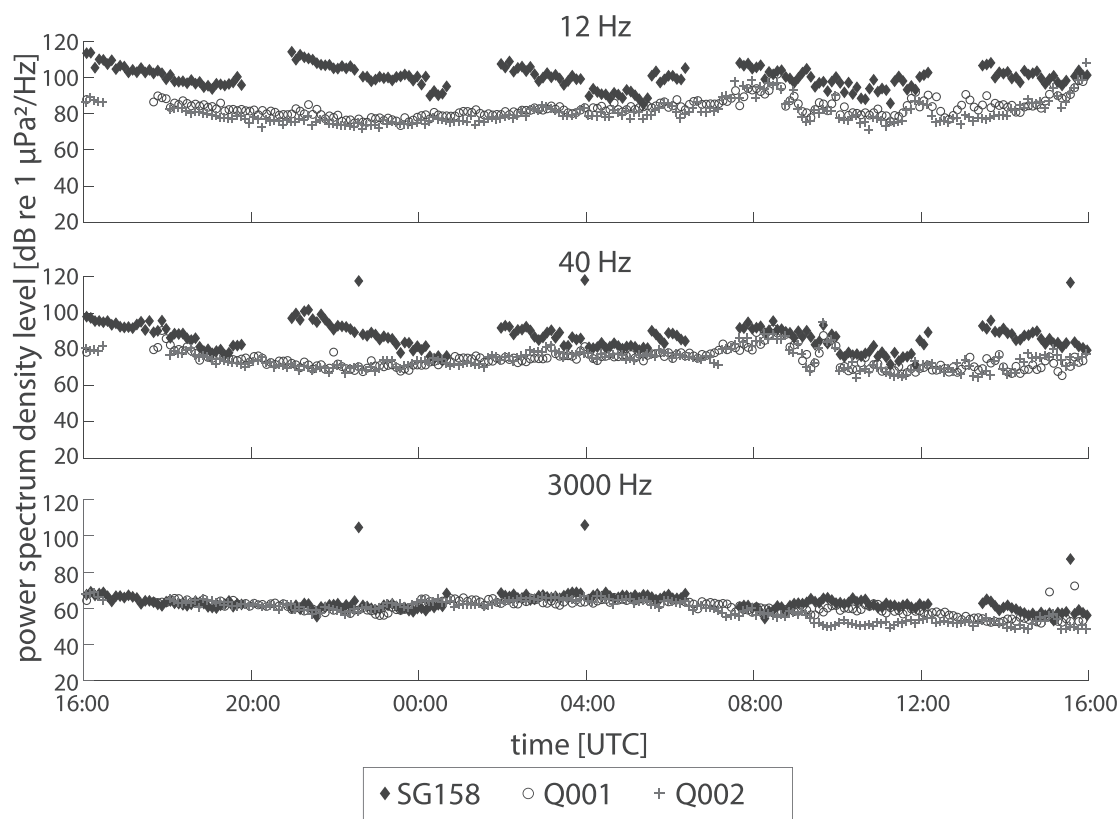


FIG. 7. Power spectrum density levels at 12, 40, and 3000 Hz for all three mobile platforms for a 24-h period from 12/26/2015 16:00 to 12/27/2015 16:00 UTC (same 24-h period shown in Fig. 5). Each point represents the lowest power spectrum density level calculated over a 10 s Hann window, each sixth minute of the 24-h period where the PAM system was active. Every sixth minute was selected to reduce the clutter of the plot. During relatively quiet periods (e.g., 16:00–03:00) the glider (solid diamonds) minimum power spectrum density levels at 12 and 40 Hz are shown to decrease over a given dive, decreasing to levels similar to the QUEphones (open circles and plus signs), while levels at 3000 Hz match those of the QUEphones, regardless of dive state. Intermittent extreme high values at the ends and middle of dives indicate times when the glider or QUEphone pump was on. Gaps in points align with time periods where the PAM system was off.

TABLE V. Regression model outputs of the final preferred model at each frequency of interest. Speed through water (stw) was calculated as vertical velocity divided by the sine of the pitch angle and is the median value for each 30-min bin. Dive state (ds) is a categorical variable including descent (negative vertical velocity) and ascent (positive vertical velocity). Time is the start time of each 30-minute bin, in minutes from the start of the first dive. The two-way interaction between speed through water and dive state is given as stw:ds.

Variable	Coefficient	Standard error	t-value	p-value
<b>12 Hz</b>				
intercept	65.2357	1.1453	56.9582	<0.0001
speed through water	1.2975	0.0497	26.1131	<0.0001
dive state (descent)	14.5623	1.5009	9.7021	<0.0001
stw:ds	-0.6434	0.0547	-11.7566	<0.0001
<b>40 Hz</b>				
intercept	77.6547	1.5129	51.3286	<0.0001
speed through water	0.3392	0.0581	5.8438	<0.0001
dive state (descent)	-7.5296	1.7210	-4.3750	<0.0001
time	-0.0002	0.0001	-3.0990	0.0021
stw:ds	0.2624	0.0623	4.2121	<0.0001
<b>3000 Hz</b>				
intercept	67.8095769	2.13206686	31.80462	0.0000
dive state (descent)	1.5043378	0.19656322	7.653201	0.0000
time	-0.00056391	0.00031836	-1.771291	0.0772

to be further adjusted for the times in which the glider or QUEphone buoyancy pump operates (less than 10 min or ~3% of total recording time per dive), which masks any possible detections during that time (Matsumoto *et al.*, 2015).

Deployment-scale detector performance was not negatively affected by glider or float platform self-noise (motor or flow noise), but this finding is specific to the low-frequency, relatively long duration and regular calling bouts of this study’s target species. The near-zero false alarm rate observed during glider descents, when flow noise was greatest, was conceivably because any faint or reflected calls were masked from detection by the detector and the manual observer. Precision will still need to be assessed on a species, call-type, and detector/deployment basis since transient broadband platform noise may cause false detections of transient broadband marine mammal sounds, like echolocation clicks.

Hour-to-hour variability in detector performance observed on both mobile and stationary recorders was likely due to the highly variable, weather-related, 10–5000 Hz soundscape (ambient sound levels) observed during the deployment, and because of the near-constant fin whale calling that sometimes resulted in a “chorus band” around

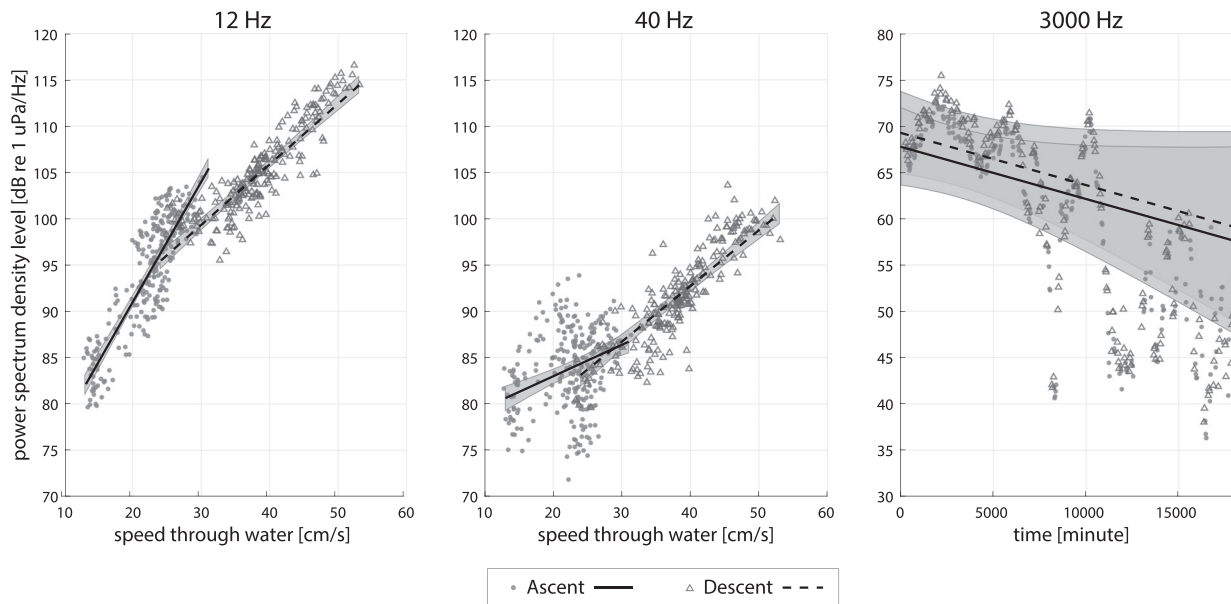


FIG. 8. Prediction plots for final regression models at each frequency. For 12 Hz (left plot) and 40 Hz (center plot), power spectrum density levels are plotted against glider speed through water for ascents (filled circles) and descents (open triangles). Lines are predicted flow noise levels with changes in speed through water in 1 cm/s intervals at each dive state (ascent—solid line, descent—dotted line), with 95% confidence intervals shaded around each line. For 3000 Hz, because speed through water was not included in the final model, power spectrum density levels are plotted against time in minutes from start of deployment.

20 Hz. This hour-to-hour variability likely explains why differences in precision were significant only between glider ascents and descents, but not between the glider (all dive states), floats, and M3R. Variability in recording conditions can alter detector performance and discussions of the assessment and reliability of detector performance over long-term datasets spanning multiple seasons, different soundscapes, and particularly between and within analysts is ongoing (Leroy *et al.*, 2018; Širović, 2016). Because the glider is likely subject to non-constant recording conditions, it is important that that detector performance is thoroughly characterized when detectors are used to analyze mobile-platform collected data.

Increased low frequency flow noise during the glider’s descending phase essentially decreased the maximum detection range of the glider relative to its detection range in only ambient noise. For example, we could model a simple theoretical scenario and calculate the range,  $r$ , over which a 15–23 Hz fin whale call could be detected, in 20 m depth bins from 200 to 1000 m, using the sonar equation

$$RL_d = SL - 15 \log_{10}(r) - t,$$

where  $RL_d$  is the received level in the 15–23 Hz band at depth bin  $d$ ,  $SL$  is source level estimated as 189 dB re 1  $\mu$ Pa at 1 m (Weirathmueller *et al.*, 2013), and  $t$  is the detection threshold, here 11 dB SNR over the 95th percentile noise level. This equation assumes a 1000 m deep, flat-bottomed environment with propagation loss due only to spreading at an intermediate rate between spherical and cylindrical (Urlick, 1983), with negligible absorption. Maximum detection radius decreased up to 97% during descents compared to ascents, within the same depth bin (Fig. 9). Conversely,

we found no correlation between platform depth and number of calls detected per hour for either the QUEphones or the glider. This was somewhat surprising given the relatively shallow calling depth of fin whales (Stimpert *et al.*, 2015) and given that such depth-dependence has been observed in monitoring beaked whales (Gkikopoulou, 2018). It is possible there were depth-dependent effects above 200 m where

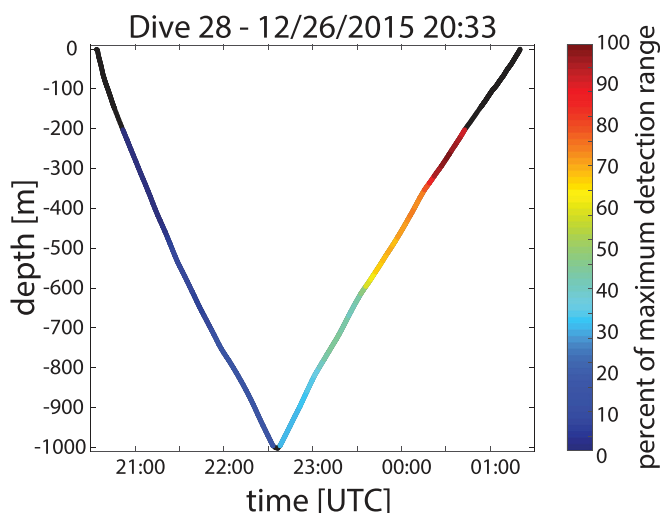


FIG. 9. (Color online) Theoretical maximum detection range over the duration of a single glider dive, Dive 28, on 12/26/2015 at 20:33 UTC. Estimated maximum detection range was calculated every 20 m of glider depth based on a call source level of 189 dB re 1  $\mu$ Pa (Weirathmueller *et al.*, 2013), transmission loss at an intermediate rate between spherical and cylindrical spreading [ $15 \cdot \log_{10}(r)$ ; Urlick (1983)], a detection threshold of 11 dB SNR, and the noise level as the 95th percentile level in that 20 m bin. Detection ranges were then normalized as a percent of the maximum detection range within the dive.

the mobile platforms did not record. This theoretical change in detection range, and the number of detections per hour, was not because of propagation differences of low frequency sounds at depths below 200 m or the shape of the sound speed profile, but instead solely because of the increased flow noise on the glider. Platform depth likely did not affect detection of fin whale calls below 200 m due to their low frequency and omnidirectional nature.

The difference in area and time surveyed by the glider due to flow noise was not anticipated and the resulting pattern appears specific to this deployment, rather than to all surveys or Seagliders. While [dos Santos et al. \(2016\)](#) reported similarly high levels of low-frequency flow noise, they did not compare differences across dive state. Increased flow noise during descents in our study was opposite that observed by [Matsumoto et al. \(2015\)](#) where a similarly equipped Seaglider showed increased flow noise during ascents. Therefore, we do not recommend altering the recording schedule to coincide only with glider ascents. Rather, attempts to mitigate flow noise should be made at the glider piloting stage by increasing dive durations and reducing thrust to decrease the glider's vertical speed during both dive states.

This difference in this study and [Matsumoto et al. \(2015\)](#) was likely due to differences in glider buoyancy and centers of mass compared to the local water density profile, not differences in piloting parameters. The same pilots flew both deployments using standard speeds and settings typical for oceanographic research. This highlights the critical importance of proper glider ballasting along with efficient, slow flight. If the glider is not properly ballasted for the water conditions in the survey area, the pilot may not have the ability to finely control the glider's descent or ascent rate throughout the mission. If it is not properly ballasted, the glider may need to perform more rolling or pitching maneuvers, creating excessive self-noise. Further, while the pilot can fly the glider at slow ascent and descent rates, it does so at the cost of forward progress. In areas with strong ocean currents, or complex pycnoclines, achieving the target speed and/or maintaining the survey plan may not be possible. Proper preparation and glider testing, as well as knowledge of the oceanographic conditions for the survey area, are essential steps in a successful and efficient glider deployment.

Because overall glider speed is difficult to accurately measure in practice ([Van Uffelen et al., 2013](#); [Van Uffelen et al., 2016](#)), defining the glider speed at which low-frequency flow noise becomes "too much" is not trivial. For this study we used a speed-through-water calculation to examine the effects of pitch and vertical velocity together. However, speed through water is not a programmable setting for the Seaglider. Instead, pitch and vertical velocity must be set individually (and even those are set through a suite of other parameters and then calculated and selected by the glider system). Speed through water varies by both vertical velocity (adjusted by changes in buoyancy) and pitch (adjusted by shifting the glider's center of mass). If pitch is held constant, increasing vertical velocity increases the speed through water. Conversely, if vertical velocity is held constant, increasing the

pitch decreases speed through water. High vertical velocities with high pitches would result in the same speed through water as a low vertical velocity and low pitch angle. Based on our regression analysis and visual inspection of the data, keeping speed through water below 25 cm/s should minimize flow noise (Fig. 8). In looking towards future Seaglider surveys, we conservatively suggest 10 cm/s vertical velocity and pitch angles of around 30° as the preferred flight parameters to limit flow noise that may reduce a recorder's detection range for marine mammal calls of interest below 60 Hz (Fig. 5). Vertical velocities of 10 cm/s match the recommended value for maximum efficiency of Seaglider flight ([School of Oceanography and Applied Physics Laboratory, 2011](#)). If vertical velocities of 10 cm/s are not possible due to ballasting or local oceanographic conditions, then pitch should be increased to try to counter act the increased vertical velocity, although this will decrease the total distance over ground traveled per dive.

Neither QUEphone exhibited any flow noise, which was expected since the QUEphones drifted with the water and currents, rather than through or against it. While flow noise could be possible during QUEphone ascents and descents, it appears unlikely since typical ascent and descent speeds are less than 10 cm/s (ascending or descending 1000 m over 3–4 h). Testing of greater ascent and descent speeds would be needed to investigate this further. The QUEphone hydrophone placement differed from SG158, with the hydrophone mounted on the top of the float while the glider's hydrophone was on the tapered aft portion. While hydrophone placement could influence flow noise generation, we do not expect that is the reason flow noise was not observed on the QUEphones but was on the glider. The glider's aft hull hydrophone placement surely placed it in a region prone to the turbulence of vortex shedding, but as the regression analysis showed, speed is an important component to flow noise generation. Future comparisons of different glider hydrophone placement may provide improvements to the flow noise observed here.

Our findings show that in future work estimating density of low-frequency animals from moving platforms, it will be critical to assess how call detectability changes with recorder depth and dive state, ideally on a per-survey basis. Call detectability could be influenced not only by platform-generated flow noise, but also because a vertical profiling glider or float is moving up and down through local oceanographic conditions and stratification that affect sound propagation. If minimum glider speeds cannot be maintained due to local oceanographic conditions such as changes in water density and currents, survey effort could be adjusted to focus only on periods when low frequency noise levels are within an appropriate threshold, or detection probability could be modeled with glider dive state as a covariate. Further, the effect of glider flow noise will need to be reassessed for higher-frequency vocalizing marine mammals such as odontocetes, as the elevated noise level on dive descents was negligible above a few hundred Hz and glider speed had no effect on noise levels at 3000 Hz.

## V. CONCLUSION

Underwater gliders and deep-water profiling floats provide a novel method for passive acoustic monitoring of low frequency marine mammal species. The survey capabilities of these platforms are different than stationary, bottom moored recorders. Overall assessment of animal presence and absence, at the hourly and daily scales, did not vary between a stationary, bottom-moored system and a mobile platform. The difference in rates of detection of individual calls observed on the glider was tightly coupled with increased flow noise levels caused by increased glider vertical speed. We quantified these differences and identified how these differences need to be addressed or can be mitigated in future work on estimating animal density and abundance from slow-moving acoustic platforms such as gliders and floats.

We propose that gliders and floats are efficient platforms for recording and detecting low frequency marine mammal vocalizations such as 20 Hz fin whale calls. Because detection capabilities are comparable to other methods, they could be used in conjunction with different recorder types (e.g., moored recorders, surface drifters, or towed arrays) to comprehensively survey an area of interest. The glider allowed us to survey a large area with a single hydrophone and the dual deployment of two QUEphones provided moderate spatial coverage of the area of interest. Despite differences in total detections on the glider, overall detectability of fin whale calls was high, and hourly and daily presence were consistent with the stationary recorders. However, much work is still needed to apply differences in calls detected and survey effort to estimate density and abundance and to conduct similar comparisons across a range of marine mammal vocalization types.

## ACKNOWLEDGMENTS

The authors thank Alex Turpin for his work on implementing the acoustic system on the glider and floats and for his help in the field, Ronald Morrissey and the crew of the *RSC4* for assistance with the field work, and Anatoli Erofeev for glider piloting services and expertise. We thank Mark Baumgartner, two additional anonymous reviewers, and Ari Friedlaender and Selina Heppell (SF's Ph.D. Committee) for their thoughtful review and feedback on the manuscript. Funding for this work was provided by the Living Marine Resources Program Grant No. N39430-14-C-1435 and Office of Naval Research Grant No. N00014-15-1-2142. S.F. was supported by the National Science and Engineering Graduate Fellowship. This is PMEL Contribution No. 4932.

<sup>1</sup>See supplementary material at <https://doi.org/10.1121/10.0000617> for additional data tables and figures. Data includes normalized hourly detection counts of fin whale 20 Hz pulses for all mobile and stationary recorders. Additional figures include LTSAs of the full deployment for all three mobile instruments, the SNR distribution of detections and Kruskal-Wallis test outputs for the detector assessment, variation in M3R detections per hour across all M3R hydrophones, and exploratory and residual plots for the regression analysis.

Barlow, J., Griffiths, E. T., Klinck, H., and Harris, D. V. (2018). "Diving behavior of Cuvier's beaked whales inferred from three-dimensional acoustic localization and tracking using a nested array of drifting hydrophone recorders," *J. Acoust. Soc. Am.* **144**, 2030–2041.

Barlow, J., Rankin, S., and Dawson, S. (2008). "A guide to constructing hydrophones and hydrophone arrays for monitoring marine mammal vocalizations," NOAA Technical Memorandum NOAA-TM-NMFS-SWFSC-417, available from NOAA Southwest Fisheries Science Center, La Jolla, CA.

Barnes, C. R., Best, M. M. R., Bornhold, B. D., Juniper, S. K., Pirenne, B., and Phibbs, P. (2007). "The NEPTUNE Project—A cabled ocean observatory in the NE Pacific: Overview, challenges and scientific objectives for the installation and operation of Stage I in Canadian waters," in *2007 Symposium on Underwater Technology and Workshop on Scientific Use of Submarine Cables and Related Technologies*, IEEE, pp. 308–313.

Baumgartner, M. F., and Fratantoni, D. M. (2008). "Diel periodicity in both sei whale vocalization rates and the vertical migration of their copepod prey observed from ocean gliders," *Limnol. Oceanogr.* **53**, 2197–2209.

Baumgartner, M. F., Fratantoni, D. M., Hurst, T. P., Brown, M. W., Cole, T. V. N., Van Parijs, S. M., and Johnson, M. P. (2013). "Real-time reporting of baleen whale passive acoustic detections from ocean gliders," *J. Acoust. Soc. Am.* **134**, 1814–1823.

Baumgartner, M. F., Stafford, K. M., and Latha, G. (2018). "Near real-time underwater passive acoustic monitoring of natural and anthropogenic sounds," in *Observing the Oceans in Real Time*, edited by R. Vankatesan, A. Tandon, E. D'Asaro, and M. A. Atmanand (Springer, Berlin), pp. 203–226.

Bittencourt, L., Soares-Filho, W., de Lima, I. M. S., Pai, S., Lailson-Brito, J., Barreira, L. M., Azevedo, A. F., and Guerra, L. A. A. (2018). "Mapping cetacean sounds using a passive acoustic monitoring system towed by an autonomous Wave Glider in the Southwestern Atlantic Ocean," *Deep Sea Res. Part I Oceanogr. Res. Pap.* **142**, 58–68.

Bray, N. A., Keyes, A., and Morawitz, W. M. L. (2002). "The California Current system in the Southern California Bight and the Santa Barbara Channel," *J. Geophys. Res. Ocean.* **104**, 7695–7714, <https://doi.org/10.1029/1998jc900038>.

Buckland, S. T., Anderson, D. R., Burnham, K. P., Laake, J. L., Borchers, D. L., and Thomas, L. (2001). *Introduction to Distance Sampling* (Oxford University Press, Oxford).

Burnham, R. E., Duffus, D. A., and Mouy, X. (2019). "The presence of large whale species in Clayoquot Sound and its offshore waters," *Cont. Shelf Res.* **177**, 15–23.

Cauchy, P., Heywood, K. J., Merchant, N. D., Queste, B. Y., and Testor, P. (2018). "Wind speed measured from underwater gliders using passive acoustics," *J. Atmos. Ocean. Technol.* **35**, 2305–2321.

Cholewiak, D., DeAngelis, A. I., Palka, D., Corkeron, P. J., and Van Parijs, S. M. (2017). "Beaked whales demonstrate a marked acoustic response to the use of shipboard echosounders," *R. Soc. Open Sci.* **4**, 170940.

Davis, G. E., Baumgartner, M. F., Bonnell, J. M., Bell, J., Berchok, C., Bort Thornton, J., Brault, S., Buchanan, G., Charif, R. A., Cholewiak, D., Clark, C. W., Corkeron, P., Delarue, J., Dudzinski, K., Hatch, L., Hildebrand, J., Hodge, L., Klinck, H., Kraus, S., Martin, B., Mellinger, D. K., Moors-Murphy, H., Nieukirk, S., Nowacek, D. P., Parks, S., Read, A. J., Rice, A. N., Risch, D., Širović, A., Soldevilla, M., Stafford, K., Stanistreet, J. E., Summers, E., Todd, S., Warde, A., and Van Parijs, S. M. (2017). "Long-term passive acoustic recordings track the changing distribution of North Atlantic right whales (*Eubalaena glacialis*) from 2004 to 2014," *Sci. Rep.* **7**, 13460.

Davis, R., Baumgartner, M., Comeau, A., Cunningham, D., Davies, K., Furlong, A., Johnson, H., L'Orsa, S., Ross, T., Taggart, C., and Whoriskey, F. (2016). "Tracking whales on the Scotian Shelf using passive acoustic monitoring on ocean gliders," in *Oceans 2016 MTS/IEEE*, Monterey, CA.

Dong, C., Idica, E. Y., and McWilliams, J. C. (2009). "Circulation and multiple-scale variability in the Southern California Bight," *Prog. Oceanogr.* **82**, 168–190.

dos Santos, F. A., São Thiago, P. M., de Oliveira, A. L. S., Barmak, R., Lima, J. A. M., de Almeida, F. G., and Paula, T. P. (2016). "Investigating flow noise on underwater gliders acoustic data," *J. Acoust. Soc. Am.* **140**, 3409.

Dugan, P. J., Klinck, H., Roch, M. A., and Helble, T. A. (2016). "RAVEN-X: A high performance data mining toolbox for bioacoustic data



- analysis,” ONR Report No. N00014-16-1-3156, <https://arxiv.org/ftp/arxiv/papers/1610/1610.03772.pdf> (Last viewed 01/26/2020).
- Dugan, P., Zollweg, J., Roch, M., Helble, T., Pitzrick, M., Clark, C., and Klinck, H. (2018). “The Raven-X Software Package. A scalable high-performance computing framework in Matlab for the analysis of large bioacoustic sound archives,” *Zenodo*, Dataset <http://dx.doi.org/10.5281/zenodo.1221420>
- Gkikopoulou, K. C. (2018). “Getting below the surface: Density estimation methods for deep diving animals using slow autonomous underwater vehicles,” Ph.D. thesis, University of St Andrews, St Andrews, Scotland.
- Goldbogen, J. A., Calambokidis, J., Shadwick, R. E., Oleson, E. M., McDonald, M. A., and Hildebrand, J. A. (2006). “Kinematics of foraging dives and lunge-feeding in fin whales,” *J. Exp. Biol.* **209**, 1231–1244.
- Griffiths, E. T., and Barlow, J. (2016). “Cetacean acoustic detections from free-floating vertical hydrophone arrays in the southern California Current,” *J. Acoust. Soc. Am.* **140**, EL399–EL404.
- Guazzo, R. A., Helble, T. A., Weller, D. W., Wiggins, M., and Hildebrand, J. A. (2017). “Migratory behavior of eastern North Pacific gray whales tracked using a hydrophone array,” *PLoS One* **12**, e0185585.
- Guerra, M., Dawson, S. M., Brough, T. E., and Rayment, W. J. (2014). “Effects of boats on the surface and acoustic behaviour of an endangered population of bottlenose dolphins,” *Endanger. Species Res.* **24**, 221–236.
- Harris, D. V., Fregosi, S., Klinck, H., Mellinger, D. K., Barlow, J., and Thomas, L. (2017). “Evaluating autonomous underwater vehicles as platforms for animal population density estimation,” *J. Acoust. Soc. Am.* **141**, 3606.
- Hatch, L. T., Clark, C. W., Van Parijs, S. M., Frankel, A. S., and Ponirakis, D. W. (2012). “Quantifying loss of acoustic communication space for right whales in and around a US National Marine Sanctuary,” *Conserv. Biol.* **26**, 983–994.
- Helble, T. A., D’Spain, G. L., Campbell, G. S., and Hildebrand, J. A. (2013a). “Calibrating passive acoustic monitoring: Correcting humpback whale call detections for site-specific and time-dependent environmental characteristics,” *J. Acoust. Soc. Am.* **134**, EL400–EL406.
- Helble, T. A., D’Spain, G. L., Hildebrand, J. A., Campbell, G. S., Campbell, R. L., and Heaney, K. D. (2013b). “Site specific probability of passive acoustic detection of humpback whale calls from single fixed hydrophones,” *J. Acoust. Soc. Am.* **134**, 2556–2570.
- Helble, T. A., Henderson, E. E., Ierley, G. R., and Martin, S. W. (2016). “Swim track kinematics and calling behavior attributed to Bryde’s whales on the Navy’s Pacific Missile Range Facility,” *J. Acoust. Soc. Am.* **140**, 4170–4177.
- Hickey, B. M. (2003). “Local and remote forcing of currents and temperature in the central Southern California Bight,” *J. Geophys. Res.* **108**, 1–26, <https://doi.org/10.1029/2000jc000313>.
- Hildebrand, J. (2009). “Anthropogenic and natural sources of ambient noise in the ocean,” *Mar. Ecol. Prog. Ser.* **395**, 5–20.
- Hildebrand, J. A., Baumann-Pickering, S., Frasier, K. E., Trickey, J. S., Merken, K. P., Wiggins, S. M., McDonald, M. A., Garris, L. P., Harris, D., Marques, T. A., and Thomas, L. (2015). “Passive acoustic monitoring of beaked whale densities in the Gulf of Mexico,” *Sci. Rep.* **5**, 16343.
- Holt, M. M., Noren, D. P., Veirs, V., Emmons, C. K., and Veirs, S. (2009). “Speaking up: Killer whales (*Orcinus orca*) increase their call amplitude in response to vessel noise,” *J. Acoust. Soc. Am.* **125**, EL27–EL32.
- Ierley, G., and Helble, T. A. (2016). “Fin whale call sequence analysis from tracked fin whales on the Southern California Offshore Range,” *J. Acoust. Soc. Am.* **140**, 3295.
- Ioup, G. E., Ioup, J. W., Sidorovskaia, N. A., Tiemann, C. O., Kuczaj, S. A., Ackleh, A. S., Newcomb, J. J., Ma, B., Paulos, R., Ekimov, A., Rayborn, G. H., Jr., Stephens, J. M., and Tashmukhambetov, A. M. (2016). “Environmental Acoustic Recording System (EARS) in the Gulf of Mexico,” in *Listening in the Ocean*, edited by W. W. L. Au and M. O. Lammers (Springer, New York), pp. 117–162.
- Jarvis, S. M., Morrissey, R. P., Moretti, D. J., DiMarzio, N. A., and Shaffer, J. A. (2014). “Marine Mammal Monitoring on Navy Ranges (M3R): A toolset for automated detection, localization, and monitoring of marine mammals in open ocean environments,” *Mar. Technol. Soc. J.* **48**, 5–20.
- Johnson, M., Madsen, P. T., Zimmer, W. M. X., Aguilar de Soto, N., and Tyack, P. L. (2004). “Beaked whales echolocate on prey,” *Proc. R. Soc. B. Biol. Sci.* **271**, S383–S386.
- Klinck, H., Fregosi, S., Matsumoto, H., Turpin, A., Mellinger, D. K., Erofeev, A., Barth, J. A., Shearman, R. K., Jafarmadar, K., and Stelzer, R. (2016). “Mobile autonomous platforms for passive-acoustic monitoring of high-frequency cetaceans,” in *Robotic Sailing 2015*, edited by A. Friebe and F. Haug (Springer International Publishing, Cham), pp. 29–37.
- Klinck, H., Mellinger, D. K., Klinck, K., Bogue, N. M., Luby, J. C., Jump, W. A., Shilling, G. B., Litchendorf, T., Wood, A. S., Schorr, G. S., and Baird, R. W. (2012). “Near-real-time acoustic monitoring of beaked whales and other cetaceans using a Seaglider™,” *PLoS One* **7**, e36128.
- Klinck, H., Nieuwirk, S. L., Fregosi, S., Klinck, K., Mellinger, D. K., Lastuka, S., Shilling, G. B., and Luby, J. C. (2015). “Cetacean studies in the Mariana Islands Range Complex in March–April 2015: Passive acoustic monitoring of marine mammals using gliders final report,” prepared for Commander, U.S. Pacific Fleet, Environmental Readiness Division, Pearl Harbor, HI, submitted to Naval Facilities Engineering Command (NAVFAC) Pacific, Pearl Harbor, Hawaii under Contract No. N62470-10-D-3011, Task Order KB25, issued to HDR Inc., Honolulu, Hawaii. August 2015 [http://www.navy.marinespeciesmonitoring.us/files/1314/4530/3483/App\\_C-Klinck\\_et\\_al\\_2015\\_Cetacean\\_Studies\\_in\\_MIRC\\_Sept-Nov\\_2014\\_PAM\\_Using\\_Gliders.pdf](http://www.navy.marinespeciesmonitoring.us/files/1314/4530/3483/App_C-Klinck_et_al_2015_Cetacean_Studies_in_MIRC_Sept-Nov_2014_PAM_Using_Gliders.pdf) (Last viewed 01/26/2020).
- Küsel, E. T., Mellinger, D. K., Thomas, L., Marques, T. A., Moretti, D., and Ward, J. (2011). “Cetacean population density estimation from single fixed sensors using passive acoustics,” *J. Acoust. Soc. Am.* **129**, 3610–3622.
- Küsel, E. T., Munoz, T., Siderius, M., Mellinger, D. K., and Heimlich, S. (2017). “Marine mammal tracks from two-hydrophone acoustic recordings made with a glider,” *Ocean Sci.* **13**, 273–288.
- Lammers, M. O., Brainard, R. E., Au, W. W. L., Mooney, T. A., and Wong, K. B. (2008). “An ecological acoustic recorder (EAR) for long-term monitoring of biological and anthropogenic sounds on coral reefs and other marine habitats,” *J. Acoust. Soc. Am.* **123**, 1720–1728.
- Leroy, E. C., Thomisch, K., Royer, J.-Y., Boebel, O., and Van Opzeeland, I. (2018). “On the reliability of acoustic annotations and automatic detections of Antarctic blue whale calls under different acoustic conditions,” *J. Acoust. Soc. Am.* **144**, 740–754.
- Lesage, V., Barrette, C., Kingsley, M. C. S., and Sjare, B. (1999). “The effect of vessel noise on the vocal behavior of belugas in the St Lawrence River Estuary, Canada,” *Mar. Mammal Sci.* **15**, 65–84.
- Lillis, A., Caruso, F., Mooney, T. A., Llopiz, J., Bohnenstiehl, D., and Eggleston, D. B. (2018). “Drifting hydrophones as an ecologically meaningful approach to underwater soundscape measurement in coastal benthic habitats,” *J. Ecoacoustics* **2**, STBDH1.
- Marques, T. A., Thomas, L., Martin, S. W., Mellinger, D. K., Ward, J. A., Moretti, D. J., Harris, D., and Tyack, P. L. (2013). “Estimating animal population density using passive acoustics,” *Biol. Rev.* **88**, 287–309.
- Marques, T. A., Thomas, L., Ward, J., DiMarzio, N., and Tyack, P. L. (2009). “Estimating cetacean population density using fixed passive acoustic sensors: An example with Blainville’s beaked whales,” *J. Acoust. Soc. Am.* **125**, 1982–1994.
- Matsumoto, H., Dziak, R. P., Mellinger, D. K., Fowler, M., Haxel, J., Lau, A., Meinig, C., Bumgardner, J., and Hannah, W. (2006). “Autonomous hydrophones at NOAA/OSU and a new seafloor sentry system for real-time detection of acoustic events,” in *Oceans 2006, MTS/IEEE*.
- Matsumoto, H., Haxel, J., Turpin, A., Fregosi, S., Mellinger, D. K., Fowler, M. J., Baumann-Pickering, S., Dziak, R. P., Klinck, H., Klinck, K., Erofeev, A., Barth, J. A., Shearman, R. K., and Jones, C. (2015). “Simultaneous operation of mobile acoustic recording systems off the Washington Coast for cetacean studies: System noise level evaluations,” *Oceans 2015, MTS/IEEE*.
- Matsumoto, H., Jones, C., Klinck, H., Mellinger, D. K., Dziak, R. P., and Meinig, C. (2013). “Tracking beaked whales with a passive acoustic profiler float,” *J. Acoust. Soc. Am.* **133**, 731–740.
- Mellinger, D., and Barlow, J. (2003). “Future directions for acoustic marine mammal surveys: Stock assessment and habitat use,” report of a workshop held in La Jolla, CA, 20–22 November, 2002, <https://www.pmel.noaa.gov/pubs/PDF/mell2557/mell2557.pdf> (Last viewed 01/26/2020).
- Mellinger, D. K., and Bradbury, J. W. (2007). “Acoustic measurement of marine mammal sounds in noisy environments,” in *Proceedings of the Second International Conference on Underwater Acoustic Measurements: Technologies and Results*, Heraklion, Greece, 25–29 June, 2007, <ftp://ftp.pmel.noaa.gov/newport/mellinger/papers/Mellinger+Bradbury07-BioacousticMeasurementInNoise-UAM,Crete.pdf> (Last viewed 01/26/2020).

- Mellinger, D. K., and Clark, C. W. (2000). "Recognizing transient low-frequency whale sounds by spectrogram correlation," *J. Acoust. Soc. Am.* **107**, 3518–3529.
- Mellinger, D. K., Nieuwkerk, S. L., Heimlich, S. L., Fregosi, S., Küsel, E. T., Siderius, M., and Sidorovskaia, N. (2017). "Passive acoustic monitoring in the Northern Gulf of Mexico using ocean gliders," *J. Acoust. Soc. Am.* **142**, 2533.
- Mellinger, D. K., Roch, M. A., Nosal, E.-M., and Klinck, H. (2016). "Signal Processing," in *Listening in the Ocean*, edited by W. W. L. Au and M. O. Lammers (Springer, New York), pp. 359–409.
- Mellinger, D. K., Stafford, K., Moore, S., Dziak, R. P., and Matsumoto, H. (2007). "An overview of fixed passive acoustic observation methods for cetaceans," *Oceanography* **20**, 36–45.
- Merchant, N. D., Barton, T. R., Thompson, P. M., Pirota, E., Dakin, D. T., and Dorocicz, J. (2013). "Spectral probability density as a tool for ambient noise analysis," *J. Acoust. Soc. Am.* **133**, EL262–EL267.
- Miller, P. J., and Tyack, P. L. (1998). "A small towed beamforming array to identify vocalizing resident killer whales (*Orcinus orca*) concurrent with focal behavioral observations," *Deep Sea Res. Part II Top. Stud. Oceanogr.* **45**, 1389–1405.
- Moore, S. E., Howe, B. M., Stafford, K. M., and Boyd, M. L. (2007). "Including whale call detection in standard ocean measurements: Application of acoustic Seagliders," *Mar. Technol. Soc. J.* **41**, 53–57.
- Moretti, D., Morrissey, R., Jarvis, S., and Shaffer, J. (2016). "Findings from US Navy hydrophone ranges," in *Listening in the Ocean*, edited by W. W. L. Au and M. O. Lammers (Springer, New York), pp. 239–256.
- Nieuwkerk, S. L., Fregosi, S., Mellinger, D. K., and Klinck, H. (2016). "A complex baleen whale call recorded in the Mariana Trench Marine National Monument," *J. Acoust. Soc. Am.* **140**, EL274–EL279.
- Norris, T. F., Dunleavy, K. J., Yack, T. M., and Ferguson, E. L. (2017). "Estimation of minke whale abundance from an acoustic line transect survey of the Mariana Islands," *Mar. Mammal Sci.* **33**, 574–592.
- Norris, T. F., Oswald, J. N., Yack, T. M., Ferguson, E. L., Hom-Weaver, C., Dunleavy, K., Coates, S., and Dominello, T. (2012). "An analysis of acoustic data from the Mariana Island Sea Turtle and Cetacean survey (MISTCS)," prepared for Commander, Pacific Fleet, Pearl Harbor, HI, submitted to Naval Facilities Engineering Command Pacific (NAVFAC), EV2 Environmental Planning, Pearl Harbor, HI, under contract No. N62470-10D-3011 CTO KB08, Task Order #002 issued to HDR, Inc., submitted by Bio-Waves Inc., Encinitas, CA.
- Quick, N. J., and Janik, V. M. (2012). "Bottlenose dolphins exchange signature whistles when meeting at sea," *Proc. R. Soc. B Biol. Sci.* **279**, 2539–2545.
- R Core Team (2019). "R: A language and environment for statistical computing," <https://www.r-project.org/> (Last viewed 01/26/2020).
- Rankin, S., and Barlow, J. (2005). "Source of the North Pacific 'boing' sound attributed to minke whales," *J. Acoust. Soc. Am.* **118**, 3346–3351.
- Rankin, S., Barlow, J., and Oswald, J. N. (2008). "An assessment of the accuracy and precision of localization of a stationary sound source using a two-element towed hydrophone array," NOAA Technical Memorandum NOAA-TM-NMFS-SWFSC-416.
- Rankin, S., Oswald, J. N., Barlow, J., and Lammers, M. O. (2007). "Patterned burst-pulse vocalizations of the northern right whale dolphin, *Lissodelphis borealis*," *J. Acoust. Soc. Am.* **121**, 1213–1218.
- Roch, M. A., Batchelor, H., Baumann-Pickering, S., Berchok, C. L., Cholewiak, D., Fujioka, E., Garland, E. C., Herbert, S., Hildebrand, J. A., Oleson, E. M., Van Parijs, S., Risch, D., Širović, A., and Soldevilla, M. (2016). "Management of acoustic metadata for bioacoustics," *Ecol. Inform.* **31**, 122–136.
- Roemmich, D., Johnson, G., Riser, S., Davis, R., Gilson, J., Owens, W. B., Garzoli, S. L., Schmid, C., and Ignaszewski, M. (2009). "The Argo Program: Observing the global oceans with profiling floats," *Oceanography* **22**, 34–43.
- Rudnick, D. L., Davis, R. E., Eriksen, C. C., Fratantoni, D. M., and Perry, M. J. (2004). "Underwater gliders for ocean research," *Mar. Technol. Soc. J.* **38**, 48–59.
- School of Oceanography and Applied Physics Laboratory (2011). "Seaglider Pilot's Guide," University of Washington, [http://gliderfs.coas.oregonstate.edu/sgliderweb/Seaglider\\_Pilot's\\_Guide.pdf](http://gliderfs.coas.oregonstate.edu/sgliderweb/Seaglider_Pilot's_Guide.pdf) (Last viewed 01/26/2020).
- Širović, A. (2016). "Variability in the performance of the spectrogram correlation detector for north-east Pacific blue whale calls," *Bioacoustics* **25**, 145–160.
- Širović, A., Hildebrand, J. A., and Wiggins, S. M. (2007). "Blue and fin whale call source levels and propagation range in the Southern Ocean," *J. Acoust. Soc. Am.* **122**, 1208–1215.
- Sousa-Lima, R. S., Norris, T. F., Oswald, J. N., and Fernandes, D. P. (2013). "A review and inventory of fixed autonomous recorders for passive acoustic monitoring of marine mammals," *Aquat. Mamm.* **39**, 23–53.
- Stafford, K. M., Mellinger, D. K., Moore, S. E., and Fox, C. G. (2007). "Seasonal variability and detection range modeling of baleen whale calls in the Gulf of Alaska, 1999–2002," *J. Acoust. Soc. Am.* **122**, 3378–3390.
- Stimpert, A. K., DeRuiter, S. L., Flacone, E. A., Joseph, J., Douglas, A. B., Moretti, D. J., Friedlaender, A. S., Calambokidis, J., Gailey, G., Tyack, P. L., and Goldbogen, J. A. (2015). "Sound production and associated behavior of tagged fin whales (*Balaenoptera physalus*) in the Southern California Bight," *Anim. Biotelemetry* **3**, 23.
- Thode, A. (2004). "Tracking sperm whale (*Physeter macrocephalus*) dive profiles using a towed passive acoustic array," *J. Acoust. Soc. Am.* **116**, 245–253.
- Thomas, L., and Marques, T. A. (2012). "Passive acoustic monitoring for estimating animal density," *Acoust. Today* **8**, 35–44.
- Van Parijs, S. M., Clark, C. W., Sousa-Lima, R. S., Parks, S. E., Rankin, S., Risch, D., and Van Opzeeland, I. C. (2009). "Management and research applications of real-time and archival passive acoustic sensors over varying temporal and spatial scales," *Mar. Ecol. Prog. Ser.* **395**, 21–36.
- Van Uffelen, L. J., Howe, B. M., Nosal, E. M., Carter, G. S., Worcester, P. F., and Dzieciuch, M. A. (2016). "Localization and subsurface position error estimation of gliders using broadband acoustic signals at long range," *IEEE J. Ocean. Eng.* **41**, 501–508.
- Van Uffelen, L. J., Nosal, E.-M., Howe, B. M., Carter, G. S., Worcester, P. F., Dzieciuch, M. A., Heaney, K. D., Campbell, R. L., and Cross, P. S. (2013). "Estimating uncertainty in subsurface glider position using transmissions from fixed acoustic tomography sources," *J. Acoust. Soc. Am.* **134**, 3260–3271.
- Van Uffelen, L. J., Roth, E. H., Howe, B. M., Oleson, E. M., and Barkley, Y. (2017). "A Seaglider-integrated digital monitor for bioacoustic sensing," *IEEE J. Ocean. Eng.* **42**, 800–807.
- von Benda-Beckmann, A. M., Lam, F. P. A., Moretti, D. J., Fulkerson, K., Ainslie, M. A., van IJsselmuide, S. P., Theriault, J., and Beerens, S. P. (2010). "Detection of Blainville's beaked whales with towed arrays," *Appl. Acoust.* **71**, 1027–1035.
- von Benda-Beckmann, A. M., Wensveen, P. J., Samara, F. I. P., Beerens, S. P., and Miller, P. J. O. (2016). "Separating underwater ambient noise from flow noise recorded on stereo acoustic tags attached to marine mammals," *J. Exp. Biol.* **219**, 2271–2275.
- Urick, R. (1983). *Principles of Underwater Sound*, 3rd ed. (Peninsula Publishing, Westport, CT).
- Verfuss, U. K., Aniceto, A. S., Harris, D. V., Gillespie, D., Fielding, S., Jiménez, G., Johnston, P., Sinclair, R. R., Siverstsen, A., Solbø, S. A., Storvold, B., and Wyatt, R. (2019). "A review of unmanned vehicles for the detection and monitoring of marine fauna," *Mar. Pollut. Bull.* **140**, 17–29.
- Ward, J. A., Jarvis, S., Moretti, D. J., Morrissey, R. P., DiMarzio, N., Johnson, M. P., Tyack, P. L., Thomas, L., and Marques, T. (2011). "Beaked whale (*Mesoplodon densirostris*) passive acoustic detection in increasing ambient noise," *J. Acoust. Soc. Am.* **129**, 662–669.
- Watkins, W. A., Tyack, P., Moore, K. E., and Bird, J. E. (1987). "The 20-Hz signals of finback whales (*Balaenoptera physalus*)," *J. Acoust. Soc. Am.* **82**, 1901–1912.
- Weirathmueller, M. J., Wilcock, W. S. D., and Soule, D. C. (2013). "Source levels of fin whale 20Hz pulses measured in the Northeast Pacific Ocean," *J. Acoust. Soc. Am.* **133**, 741–749.
- Wiggins, S. M., and Hildebrand, J. A. (2007). "High-frequency Acoustic Recording Package (HARP) for broad-band, long-term marine mammal monitoring," in *2007 Symposium on Underwater Technology and Workshop on Scientific Use of Submarine Cables and Related Technologies*, IEEE, pp. 351–357.
- Yack, T. M., Barlow, J., Calambokidis, J., Southall, B., and Coates, S. (2013). "Passive acoustic monitoring using a towed hydrophone array results in identification of a previously unknown beaked whale habitat," *J. Acoust. Soc. Am.* **134**, 2589–2595.
- Zimmer, W. M. X., Harwood, J., Tyack, P. L., Johnson, M. P., and Madsen, P. T. (2008). "Passive acoustic detection of deep-diving beaked whales," *J. Acoust. Soc. Am.* **124**, 2823–2832.
- Zuur, A. F., Ieno, E. N., Walker, N. J., Saveliev, A. A., and Smith, G. M. (2009). *Mixed Effects Models and Extensions in Ecology with R* (Springer, New York).